15 Sep 2022

A Comprehensive Review of Experimental Evaluation Methods and Results of Polymer Micro/nanogels for Enhanced Oil Recovery and Reduced Water Production

Junchen Liu

Abdulaziz Almakimi

Mingzhen Wei
Missouri University of Science and Technology, weim@mst.edu

Baojun Bai
Missouri University of Science and Technology, baib@mst.edu

et. al. For a complete list of authors, see https://scholarsmine.mst.edu/geosci_geo_peteng_facwork/2037

Recommended Citation

J. Liu et al., "A Comprehensive Review of Experimental Evaluation Methods and Results of Polymer Micro/nanogels for Enhanced Oil Recovery and Reduced Water Production," *Fuel*, vol. 324, article no. 124664, Elsevier, Sep 2022.
The definitive version is available at https://doi.org/10.1016/j.fuel.2022.124664

Fuel 324 (2022) 124664

Contents lists available at ScienceDirect

Fuel

journal homepage: www.elsevier.com/locate/fuel

Review article

A comprehensive review of experimental evaluation methods and results of polymer micro/nanogels for enhanced oil recovery and reduced water production

Junchen Liu [a], Abdulaziz Almakimi [a], Mingzhen Wei [a], Baojun Bai [a,*], Ibnelwaleed Ali Hussein [b]

[a] Department of Geosciences and Geological and Petroleum Engineering, Missouri University of Science and Technology, Rolla, MO 65409, United States
[b] College of Engineering, Qatar University, Doha, P.O. Box 2713, Qatar

ARTICLE INFO

Keywords:
Micro/nanogel
Conformance control
Evaluation method
Transport
Enhanced Oil Recovery

ABSTRACT

In recent years, polymer micro/nanogels which are re-crosslinked polymers with 3D networks, have attracted a lot of interest in Enhanced Oil Recovery (EOR) field. In size of micro/nanometers, these gel particles are designed to be conformance control agents for in-depth fluid diversion, and various experimental research have been undertaken to investigate the possibilities of applying micro/nanogels in oilfield. However, it is still unclear that how to utilize micro/nanogels to their full potential in oilfield because the transport mechanisms and EOR mechanisms of micro/nanogels are not well studied currently. By reviewing experimental evaluations and corresponding results of micro/nanogels, including evaluation of particle physiochemical properties, transport, and potential EOR mechanisms, the review aims to discuss the evaluation of micro/nanogel particles, transport issue in many experimental designs and the debates of EOR mechanisms. Finally, we present the current challenges of micro/nanogels application and recommend the future research directions based on the review.

1. Introduction

The oil development and production usually include three distinct mechanisms: primary, secondary, and tertiary (enhanced) recovery. Excessive water production is a severe issue in oil production processes worldwide. It not only decreases the oil production rate, but also increases load on surface facilities and causes corrosions [1]. As a result, the cost of per barrel of oil increases a lot. It is estimated that approximately 50 billion dollars were spent to handle excessive water production every year in the world [2,3]. Thus, solving water production problems can bring a huge benefit to oil industry.

Conformance control usually refers the methods that can be used to correct reservoir heterogeneity, through which reservoir sweep efficiency can be improved and water production can be reduced. Polymer gels have been mostly used for this purpose. Traditionally, in-situ polymer gels have been widely investigated and applied to control reservoir conformance. However, one recent interest has been focused on the development and application of microgels and nanogels in conformance control because investigators expected these tiny particles can be delivered into the in-depth of a reservoir to provide fluid flow diversion inside the reservoir rather than near wellbore [4–6]. It has been claimed that the micro/nanogels have the following advantages over traditional polymer gels. First, the gel particles can be manufactured by monomer/polymers and crosslinkers before the injection, and thus the gelation quality can be well-controlled [5,7,8]. Secondly, the particle size is controllable and can be well designed to accommodate the permeability of a target reservoir for better injectivity [9–11]. Thirdly, micro/nanogels can be better designed to be stable at harsh formation conditions, such as high temperature and high salinity compared with in-situ gels [12–14]. Finally, the particles are usually compatible with any injection water in oilfields, so they can be directly injected reservoirs by simply mixing the particles with injection water, and the injection facilities do not need to be reconstructed as shown in Fig. 1 [13,15–17], which can reduce a lot of labor costs and make the injection process very convenient.

Although micro/nanogels have drawn an increasing attention in the EOR and many studies are conducted, there are still many arguments about their EOR mechanisms, transport capacity, and application conditions. In the paper, we first review the materials and methods to synthesize these particles and the evaluation methods of their physicochemical characteristics. Then, we summarize the experimental results regarding micro/nanogel transport and retention in porous media

* Corresponding author.
E-mail address: baib@mst.edu (B. Bai).

https://doi.org/10.1016/j.fuel.2022.124664
Received 15 March 2022; Received in revised form 1 May 2022; Accepted 20 May 2022
Available online 27 May 2022

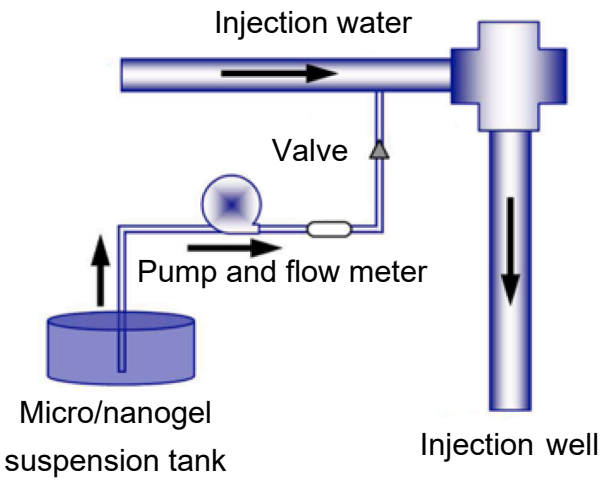

Fig. 1. Micro/nanogel injection facilities[13].

collected from literature and discuss whether these results can be used to explain the transport ability of these particles. At last, we review their EOR mechanisms and make recommendations about future research prospects.

2. Synthesis of micro/nanogels

Micro/nanogels are polymer particles that have 3D network of entangled polymer chains. These polymer chains are crosslinked by kinds of crosslinkers, and they can be synthesized by a variety of techniques. It was reported that the first microgel was the Dow Chemical 580G Lot 3584 monodisperse polystyrene, which was prepared accidently by an emulsion polymerization process in a pilot plant in 1947 [18]. Preparation of gel particles uses various ways of crosslinking, including physical cross-linking [19], chemical cross-linking [12], polymerization grafting [20] and radiation cross-linking [21]. However, chemical cross-linking is mostly used in EOR.

Divided by polymerization process, there are four major methods to synthesize micro/nanogels, including inverse emulsion polymerization, inverse suspension polymerization, dispersion polymerization and seed swelling polymerization as shown in Table 1 [22–24].

Table 2 summarizes the monomers, crosslinkers, initiators, surfactants, water phase and oil phase of the micro/nanogel synthesis. Acrylamide/2-Acrylamido-2-methylpropane sulfonic acid, N, N'-methylene bis(acrylamide) (MBAA), Ammonium persulfate/Potassium persulfate/2,2-Azobisisobutyronitrile, white oil, water, and Span80/Tween60 are commonly used as monomers, crosslinkers, initiators, oil phase, water phase and surfactants, respectively.

A variety of additives, aiming to improve thermal stability, particle strength or decorating particles, are applied in the synthesis of micro/nanogels, but the major monomer, crosslinker and initiators are AM, MBAA, and APS/KPS/AIBN, respectively, which are very commonly applied in polymer gel systems [42].

After synthesis, the chemical structure, which determines the functions and properties of micro/nanogels, are often analyzed by Fourier Transformation Infrared Spectra (FTIR), Nuclear Magnetic Resonance Spectroscopy (NMR), and elemental analysis. From Table 2, it is very common that the polymer particles are synthesized by copolymerization. FTIR and NMR are applied to make sure that the function groups or monomers are copolymerized in the polymer chains. For example, Li et al. synthesized microgel with monomers including acrylic acid (AA), arylamide (AM) and sodium p-styrene sulfonate (SSS), and the recorded FTIR spectra of monomers and microgels (named as PMs) in Fig. 2, respectively. As shown in the Fig. 2, the peaks around 984 cm^{-1} (C═C vibration), which can be seen in the first three curves, disappeared in the last one, indicating that the three monomers were polymerized [43].

Besides, NMR allows the detection of crosslinking in the microgel particles. Balaceanu et al. evaluated crosslinking distribution and heterogeneity by combining Flory Theory and ^{1}H High-Resolution Transverse Relaxation NMR [44]. Liu et al. conducted ^{1}H NMR to quantify the crosslinking of phenolic resin between amide group and hydroxyl group in microgel as shown in Fig. 3 [35]. The peak position of b was attributed to $–CH_2OH$ of phenolic resin, and the crosslinking reaction process was reflected by integral area around position b.

In addition to NMR, the elemental distribution analysis can also be used to detect some metal crosslinkers in the particles [27,31]. Wang et al. analyzed Zr in nanogel structure by using of X-ray spectroscopy, which is shown in Fig. 4.

3. Evaluation of Micro/nanogel particles

In this section, we review the evaluation methods of micro/nanogel particles, including morphology, size distribution and swelling capacity, mechanical properties, stability of dispersion and thermal stability. These are basic physicochemical features of micro/nanogels determined by their chemical structures. An accurate evaluation of these properties is essential for the application of micro/nanogels.

3.1. Morphology

The morphology is one of the most common properties for particles. Usually, the morphology observation can obtain the shape, agglomeration, initial particle size and structure of the particles. In general, optimal microscope and electron microscope are two main instruments to get the morphology of particles. Due to the diffraction limit, optimal microscope is usually used for microgels which range from 1 to 100 μm [13,16,26,31]. Initial particle size can be calculated by this method for dry particle powder (Fig. 5), and the swelling process is recorded also. Sometimes, fluorescents and dyes, such as methylene blue, are used to color the particles for better observation because swollen particles are close to transparent [45–47]. After obtaining the image, it is possible to use software like Image J to analyze the size distribution and calculate

Table 1
Summary of micro/nanogel synthesis methods.

Synthesis methods	Nucleation mechanisms	Average size range/μm	Comments
Inverse emulsion polymerization	Monomers diffuse into micelles, and micelles grow to be particles	0.06–1 Relatively wide size distribution	High polymerization rate and high polymerization degree. High surfactants amount, low solid contents.
Inverse suspension polymerization	Monomer droplets transfer into particles	0.1–5000 Wide size distribution	Simple, cheap and most preferred techniques. Particle size is less controllable.
Dispersion polymerization	Nucleation occurs when polymer chains aggregate after reaching certain length.	0.1–15 Monodispersed.	The reaction is easy to carry out. The requirements for reaction medium are very high.
Inverse microemulsion polymerization	1) nucleation in the microemulsion droplets; 2) homogeneous nucleation in the continuous phase	0.01–0.1 Narrow distribution	The reaction rate is stable. And the structure of particles is uniform and stable. High surfactant levels are needed.

Table 2
Summary of micro/nanogel synthesis chemicals.

Researcher	Monomer	Crosslinker	Initiator	Water phase	Oil phase	Surfactant
Geng et al. [25]	AETAC AM AMPS	MBAA	APS	Water	Decane	Span80 and Tween60
Wang et al.[26]	AM AMPS NVP	MBAA	KPS	Water	White oil	Span80
Liu et al.[27]	AM AMPS DAC	MBAA	KPS	Water	N/A	PDAC
Yang et al.[28]	AM AA AMPS	MBAA	APS	Water	N/A	Span80 and Tween60
Mustafa et al.[29]	AMPS	MBAA	KPS	Water	Decane	Span80 and Tween60
He et al.[10]	Styrene AM	MBAA	APS	Water	N/A	AES
He et al.[30]	AM	DVB	AIBN	Water	Acetonitrile	OP-10
Wang et al.[31]	AM AMPS NVP	MBAA and Zirconium acetate	$K_2S_2O_8$-$KHSO_3$	Water	White oil	Span80 and Tween60
Wang et al.[32]	AM	MBAA	$(NH_4)_2S_2O_8$–$NaHSO_3$	Water	White oil	Span-80 and TX-10
Yang et al.[33]	AMPS AM	MBAA and PEG	APS	Water	Aviation kerosene	Span80 and Tween60
Jia et al.[9]	AM AMPS	MBAA and PEG	AIBN	Water	Aviation kerosene	Span80 and Tween60
Zhang et al.[34]	AM 4-VBC	MBAA	AIBN	Water	DMF	N/A
Liu et al.[35]	AM AA-Na DOPA	Phenolic resin	AIBN	Water	N/A	N/A
Zhu et al.[36]	AM AMPS PEI	MBAA	N/A	N/A	N/A	N/A
Yu et al.[37]	AM AA-Na AMPS DADMAC AA-Na TBS	MBAA	KPS and Sodium bisulfite	Water	White oil	Span80 and Tween60
Gu et al.[38]	AM BA	MBAA	KPS	Water	White oil	Span80
Zhang et al.[39]	AM and AMPS	MBAA	$(NH_4)_2S_2O_8$–$NaHSO_3$	Water	White oil	Span80 Span65 Tween60 Tween80
Liang et al.[14]	α-Starch AM	MBAA	KPS	Water	N/A	N/A
Du et al.[40]	FRGO AM AMPS	MBAA	AIBN	Water	White oil	Span80 and oleic acid
Tang et al.[41]	SiO2 AM AA SSS SBMA	MBAA and PEG	APS	Water	Aviation kerosene	Span60

AA: Acrylic acid
AA-Na: Sodium Acrylate
AETAC: Acryloyloxyethyltrimethyl ammonium chloride
AES: Sodium alcohol ether sulphate
AIBN: 2,2-Azobisisobutyronitrile
AM: Acrylamide
AMPS: 2-Acrylamido-2-methylpropane sulfonic acid
APS: Ammonium persulfate
BA: Butyl Acrylate
DAC: Acryloyloxyethyl trimethyl ammonium chloride
DOPA: N-(3,4-dihydroxyphenethyl)- acrylamide
DADMAC: Dimethyl diallyl ammonium chloride
DMF: Dimethylformamide
DVB: Divinylbenzene
FRGO: Vinyl functionalized graphene oxide
KPS: Potassium persulfate
MBAA: N,N′-methylene bis(acrylamide)
NVP: *N*-Vinyl-2-pyrrolidone
OP-10: Octylphenol polyoxyethylene (10) ether
PEI: Polyethylenimine
PDAC: Polyacryloyloxyethyl trimethyl ammonium chloride
PEG: Polyethylene glycol
SBMA: [2-(methacryloyloxy) ethyl] dimethyl-(3-sulfopropyl) ammonium hydroxide
SSS: 4-Styrensulfonic acid sodium salt
TBS: 4-*tert*-butyl styrene
4-VBC: 4-vinylbenzyl chloride

the average diameter of the particles [48].

Compared with optimal microscope, electron microscope has been used to measure micro/nanogels in smaller size because it has a better resolution and magnification (Fig. 6). Emitting a beam of electron on the surface of samples, conventional SEM needs the samples to be dry and under vacuum, while the Environmental SEM allows the analysis of samples containing water, and thus the particles could be observed during the swelling process. Besides, Transmission Electron Microscope (TEM) has been used to observe nanogel particles with more details. The electron beam can transmit the samples and reveal some inner structures

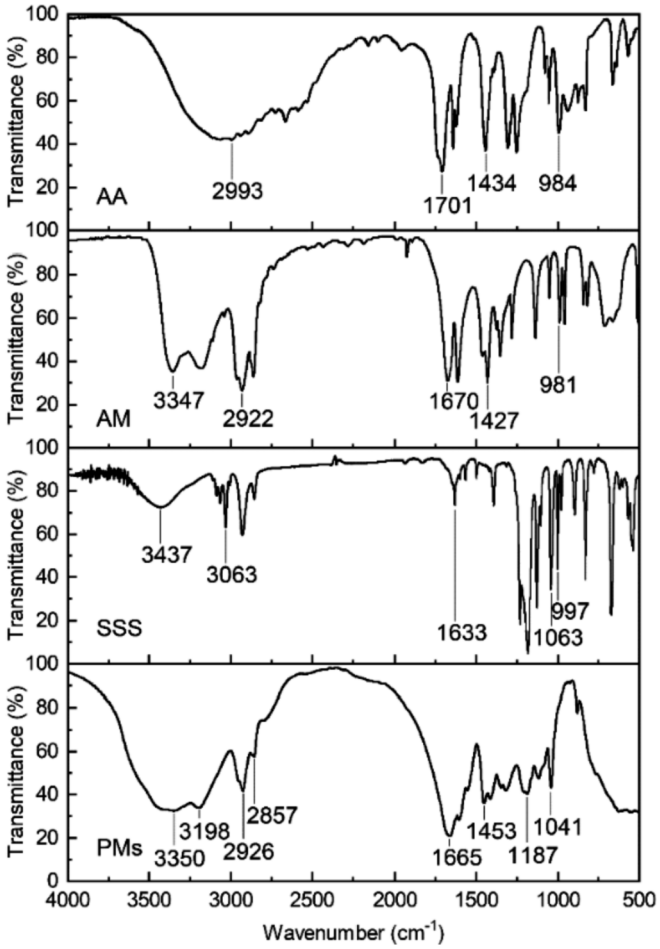

Fig. 2. FTIR spectra of the monomers and microgel[43].

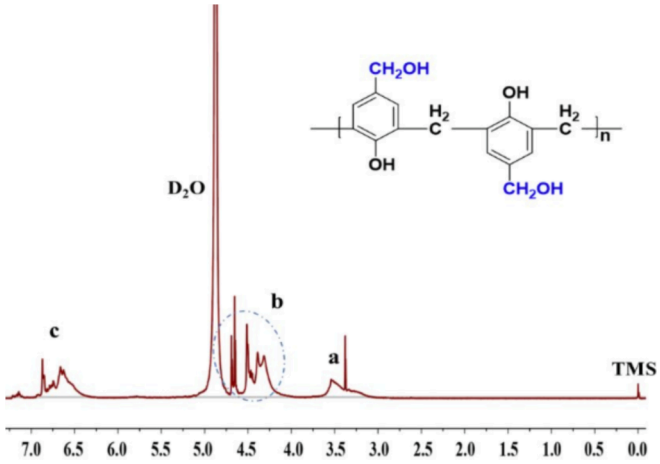

Fig. 3. ^{1}H NMR spectrum of phenolic resin [35].

of particle, such as core–shell structure. Although TEM has a better resolution than SEM and is suitable for nanogels, TEM also has higher requirements for the sample preparation. In addition, Atomic Force Microscopy (AFM) is another type of microscope, which can measure 2–3 nm in the air [50]. AFM measures the forces between the probe and the sample, and it can be used to show real 3D pictures of the surface and reveal the internal structures of particles. One of the advantages of AFM is that it does not need any special treatments, like metal coating, which enables researchers to image nonconducting surfaces. Another

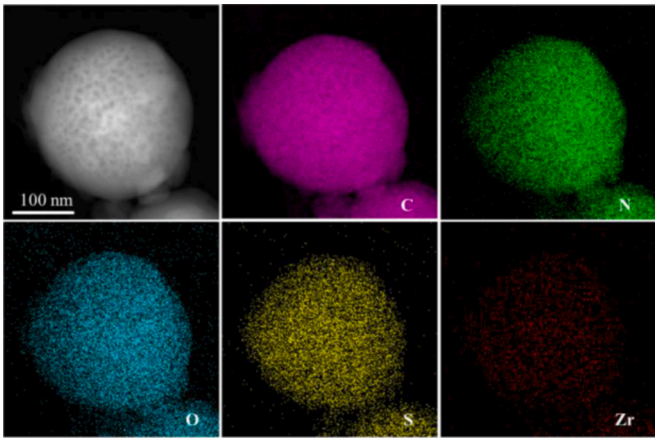

Fig. 4. High-resolution TEM images of D nanospheres particle, corresponding element maps showing the distribution of C (purple), N (green), O (blue), S (yellow), and Zr (red) [31].

Fig. 5. Macroscopic morphology of polymer microgel dry powder [49].

advantage is that AFM does not require high vacuum environment. However, its scanning image size is limited (a maximum height about 10–20 μm and scanning area of about 150 × 150 μm), and scanning speed is slower than SEM [51].

3.2. Size distribution and swelling capacity

The particle size and size distribution are the essential parameters for the micro/nanogels. As mentioned above, initial particle size can be obtained by SEM or optimal microscope. Obtaining size distribution needs computer software, such as Image J [53,54]. But it is more often to measure average size and size distribution by Dynamic Light Scattering (DLS) method. DLS is also called Photon Correlation Spectroscopy, which measures Brownian motion and relates this to the size of particles. Basically, when light hits the particles, it scatters in all directions (Rayleigh scattering), and the scattering intensity fluctuates due to the Brownian motion. The method needs to specify the viscosity of dispersion and the reflex index of particle and solution. In general, DLS method tests particles swelling at different time, different temperature and different salinity. Then the average diameter can be obtained, and the swelling capacity can be calculated. In general, there are three equations to calculate swelling ratio:

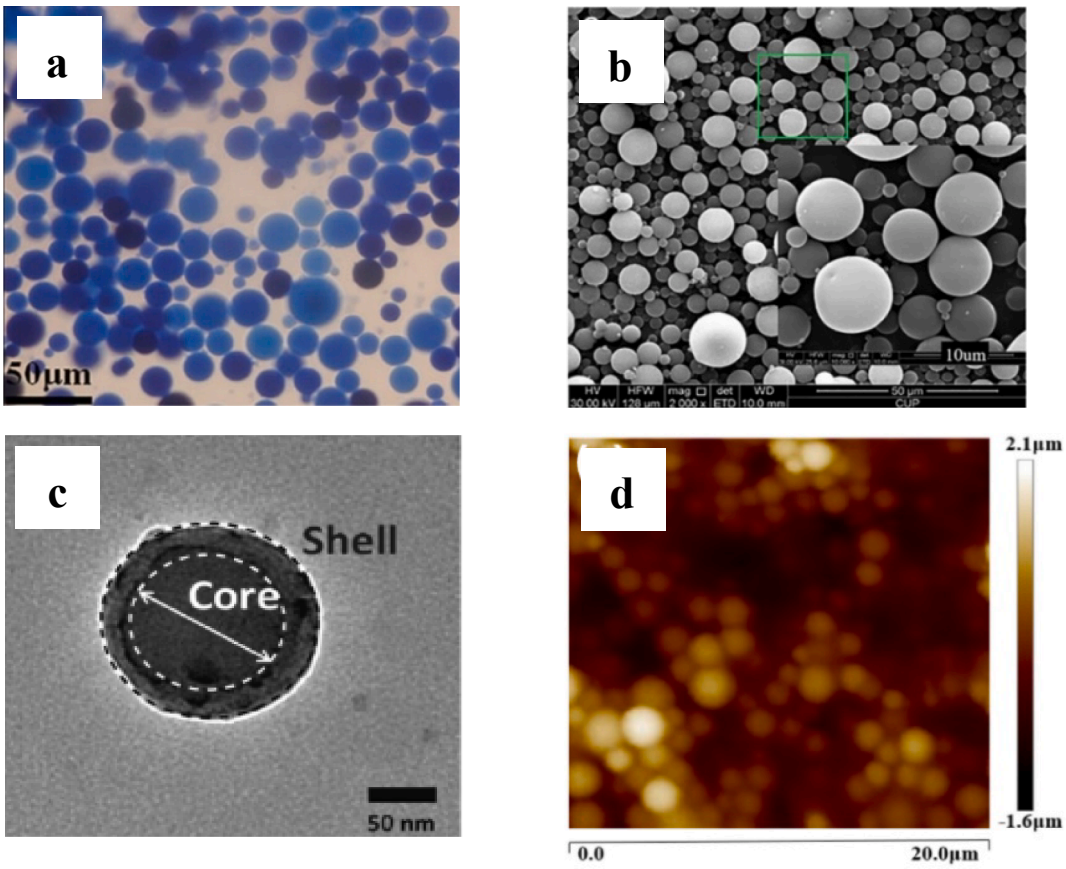

Fig. 6. (a)Methylene blue dyed microgel in optimal microscope [46]; (b)SEM photo of microgel [26]; (c)TEM photo of nanogel [52]; (d)AFM photo of microgel [35].

$$SR = \left(\frac{Dt}{d_0}\right)^3$$

where SR is the swelling ratio, $d_0$is the initial average particles size of the particles, $Dt$is the average particle size of the particles at swelling time t [26]. This is the calculation of the volume change. While the swelling ratio can also be calculated by:

$$SR = \frac{D_t - D_0}{D_0}$$

where$SR$is the swelling ratio, $D_0$is the mean particle size before the swelling, $D_t$is the mean particles size after swelling [55]. This is the

Table 3
Summary of micro/nanogel swelling capacity.

Researchers	Particles	Initial diameter/μm	Swelling ratio	Swelling time/d	Salinity/(mg/L)	Temp./℃
Li et al.[57]	Poly(AM-AMPS)/SiO2	0.05	3.42–4.12	2	0–150000	20–80
Jin et al.[59]	Graphene oxide-grafted microgel	1.98	6–9	15	0–16000	60
Liu et al.[35]	Poly(AM-AANa-DOPA)	3.5	5.14	15	14,610	80
Sun[60]	Polymer microgel	7.12	3–7.5	10	0–5000	25–65
Jia et al.[9]	Poly(AM-AMPS)	10.41	7.58	15	30000–100000	65
Zhang et al.[52]	Core-shell nanogel	0.25	6	30	37,505	50
Pu et al.[61]	Poly(AM-AMPS)	9.996	1.8–6.5	7	25,000	25–104
Wang et al.[46]	Microgel	3.51	4.85	5	9500	25
Tang et al.[41]	Polymer coated nano-SiO_2	13.6–24.6	1.71–3.62	15	0–30000	20–110
Jia et al.[62]	Polymer microgel	0.784	3.57	15	40,000	70
Hua et al.[63]	Poly(AM-AA)	0.2	3–6	5	0	82
Liu et al.[27]	Polymer coated SiO_2	1.056	2–8	15	0–15000	25–100
Yao et al.[13]	Poly(AM-APS)	12.05	1.6–2.2	10	5000	25–90
Yu et al.[37]	Polymer microgel	0.05–0.09	5.5–10.8	2–14	180,000	90
Du et al.[64]	Poly(AM-AMPS)	7.58	1.4–4.3	15	5000–20506	25–90
Liu et al.[65]	Core-shell microgel	3.3	4.06	8	2893.7	N/A
Zhao et al.[66]	Polymer nanogel	0.165 & 0.884	4.56–6.91	13	0	25
Wang et al.[26]	Poly(AM-APS-NVP)	4.1–5.58	1.42–13.85	2	0	30
Chen et al.[45]	Poly(AM-AA-AMPS)	3.1–9.8	2.68–4.34	5	0	N/A
Zhang et al[67]	Fluorescent Polyacrylamide	0.25–0.3	6–12	7	N/A	25–75
Geng et al[25]	Poly(AM) Poly(AMPS) Poly(AETAC)	0.059–0.088	2.3–3.73	1	10,000	60
He et al[10]	Poly(Styrene-AM)	0.097–0.251	1.25–1.54	0.25	0	60
Li et al[43]	Poly(AM-AA-SSS)	2.2–5.8	6.65–7.59	10	4012.7	45

calculation of the diameter change. Also, the swelling ratio can be calculated by:

$$SR = \frac{m_t - m_0}{m_0}$$

where$SR$is the swelling ratio, $m_t$is the wet weight of the swollen particles, is the dry weight of the particles [56]. This is the calculation based on mass change.

The following Table 3 lists swelling capacity of some micro/nanogels, and it shows that swelling ratio (diameter ratio) is between 1.2 and 13.8. Furthermore, since the specific surface area of the smaller particle is bigger than that of the larger particle, the smaller particle has a shorter swelling time. The swelling of polymer particles is significantly influenced by salinity and temperature, with high salinity and low temperature contributing to a low swelling ratio and swelling rate [41,57–59].

4. Swelling ratio of the table is defined as swollen diameter divided by initial diameter.

4.1. Mechanical properties of particles

Gel particles have crosslinked 3D network structures exhibiting deformation capacity. The deformation is very important to understand the transport mechanism in porous media. Basically, particle mechanical properties include elasticity and strength. Atomic Force Microscopy method, nano/micromanipulation method and bulk gel method have been used to evaluate the mechanical properties [35,56,68].

AFM experiments can provide an elastic modulus for a single particle. The principle of the experiment is physically indenting a particle with AFM probes, and the force is processed by the probe as shown in the Fig. 7. Using appropriate model, the method calculates the elastic modulus of the particle. Lei et al. used this method to calculate the elastic modulus of a microgel [56]. The slope method of Hertz model was selected for the calculation, since they believed that the contact between probe and particle was a solid-to-solid contact of elastic and isotropic materials, and the contact region was negligible compared with their bodies. However, sharp AFM can be challenging due to the tip-sample adhesion effects and the results are sensitive to imaging parameters. In addition, AFM is constrained to small deformation analysis due to lack of theoretical understanding of large deformation [69]. Therefore, there is still debate of application of Hertz model to microgel. What's more, the probe could penetrate porous crosslinked polymer rather than indenting and deforming, which needs to be identified by hysteresis in indentation curve and retract force curve [68]. Although sphere probe in AFM can have less damages on particles, the contact point of sphere probe is hard to be determined with sphere probe. In addition, it is reported that the elastic modulus could depend on the ratio of sphere probe diameter to particle diameter, which is called size effects [69]. Thus, using sphere probe is not a perfect solution for damage problem.

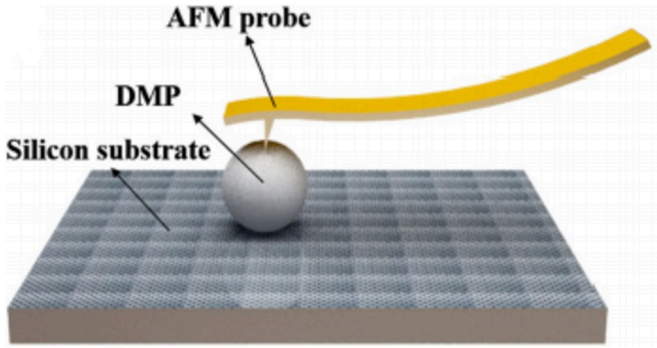

Fig. 7. A schematic diagram of the experimental setup [56].

Nano/micromanipulation method can also obtain elastic modulus, and it is able to apply higher loads and larger deformation than AFM. The principle of this new technique is to compress single particles between two flat surfaces comprising a glass slide as shown in Fig. 8 [70]. Particle deformation process is recorded by a sensitive force transducer and electron microscopes. Compared with AFM which usually has a flexible cantilever with a sharp tip, micro/nanomanipulation method is less likely to damage on the particle, and it is easier to apply a mechanical load on particles. However, the method still needs Hertz theory to explain its data, which is debatable to describe large deformation of particles. Yan et al. found that Hertz model could only explain the deformation up to 30 % using micromanipulation method [71].

Bulk gel method is a way to measure the storage modulus(G') and loss modulus(G") of single particle indirectly (Fig. 9). Usually, bulk gel is synthesized using the same chemical components with particles, and the mechanical properties can be measured very easily. Yang tested the storage modulus and creep behavior of microspheres based on bulk gel, and he also studied the effects of crosslinker concentration, initiator concentration and monomer concentration [28]. Gu measured the mechanical strength of microsphere by bulk gel in texture analyzer [38]. In the experiments, stress-stain cures were produced to evaluate particle gel strength. Overall, AFM method and micro/nanomanipulation methods provides elastic modulus, but they require a lot of preparation and expensive equipment. Bulk gel method has advantages due to its convenience and low cost, which can give storage modulus, loss modulus and stress-stain cures. But the method requires a homogenous structure of bulk gels, and it is assumed that the microgel and nanogel should exhibit the same elastic properties with bulk gels.

In addition to elasticity, microgels and nanogels should be able to resist shear stress during the injection and transport. To evaluate the shearing resistance, particles are dispersed into bine and the initial size distribution and morphology photos are taken at the beginning (Fig. 10). Then the particle dispersion will be put into high shear mixer under different shear rates. The size distribution and morphology are evaluated again after shearing. Another way is to inject dispersion into cores with high flow rates. Next, the particle size distribution and morphology are examined to compare with initial status [38]. Particle size remaining degree, which is defined by the ratio of mean particle size after shearing to the mean particle size before shearing, can be used to characterize the remaining level of particle size and mechanical stability [41].

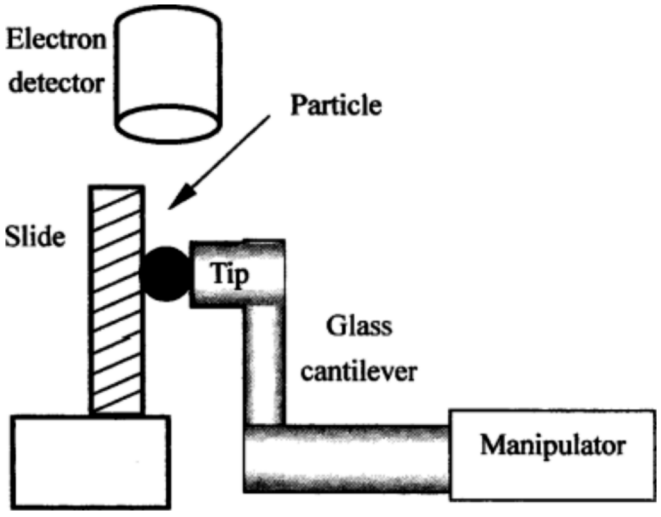

Fig. 8. Diagram of nanomanipulation device in environmental scanning electron microscope [70].

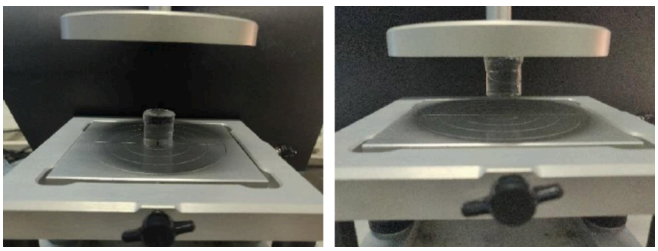

Fig. 9. Schematic diagram of compression of bulk gel sample [38].

4.2. Stability of dispersion

In-depth fluid diversion treatment requires good stability of microgel and nanogel dispersion. For a stable suspension, the particles should be well-dispersed as long as possible. The stability of suspension is influenced by many aspects, such as Brownian motion, Van der Waals attractive force, zeta potential, viscosity, gravitational force, and so on [73].

Zeta potential is very important to the nanogels, which represents the surface charge and repulsion forces between particles. According to Deryaguin–Landau–Verwey–Overbeek (DLVO) theory, nanoparticles with charge have a layer of ions (of opposite charge) strongly bound to their surface (Fig. 11). Nanoparticles with a zeta potential between − 10 and + 10 mV are considered approximately neutral, while nanoparticles with zeta potential of greater than + 30 mV or less than − 30 mV are considered strongly cationic and strongly anionic, respectively [74]. A high absolute value of zeta potential means that the repulsion forces are strong, and the particles have less agglomeration phenomenon. Sun et al. suggested that agglomeration is one of the challenges for the application of nanoparticles [75].

Sedimentation rate is one of parameters to evaluate dispersion stability. Sedimentation rate can be assessed by direct observation method and optical analysis method that uses light scattering techniques which can provide qualitative results [33,41]. The direct observation method is conducted in a transparent bottle, and particles are dispersed in brine. To have a well-dispersed suspension, the suspension is stirred and kept for a period time at certain temperature. After that, the suspension will be observed and compared with the initial status. Sedimentation phenomenon and color differences between top and bottom layer can be recorded to evaluate the suspension stability [77–80]. The method is easily to be conducted, but it cannot give us a detailed data about the stability. And uncontrolled errors are introduced when the observation is through human eyes. Thus, light scattering techniques is applied to study the stability, the principle of which has been mentioned in size distribution part. The technique can be used to analyze the rate of sedimentation or flotation phenomenon. To monitor the stability of suspension, transmittance and backscattering of pulsed light can be measured using stabilizer. The sedimentation and swelling of particles

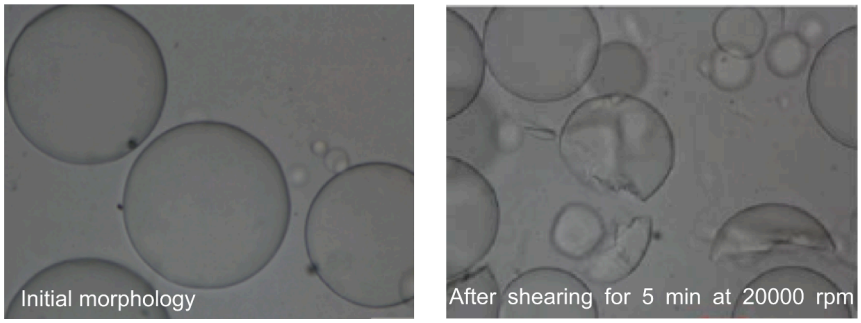

Fig. 10. Breakdown of microgel with high shear rate [72].

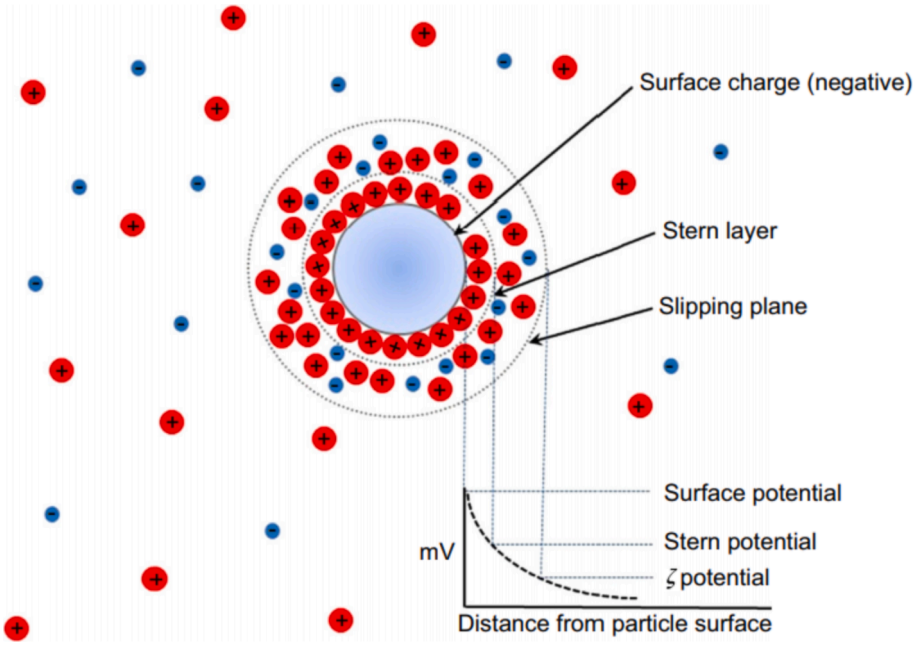

Fig. 11. Definition of zeta potential [76].

are reflected in the variation of the transmission and backscattering light intensity at different heights of the sample over time. Turbiscan Stability Index (TSI), a parameter to evaluate the stability of the dispersion system, can be generated by computer software, such as Turbisoft-Lab [41]. TSI value is defined as the following equation, and the larger the TSI value, the less stable the dispersed system is. Yang et al. depicted the relationship between the TSI value and the bottle test technique in a diagram [33,57].

$$TSI = \sqrt{\frac{\sum_{i-1}^{n}(x_i - x_{bs})}{n-1}}$$

where *TSI* represents Turbiscan Stability Index, n is the scan times, x_i is the backscattering light intensity at the scanning time of$i$, and x_{bs} is the average backscattering light intensity.

4.3. Thermal stability

The thermal stability of micro/nanogels refers to how long the particle can keep its structure and strength at high temperature and salinity. Thermal stability is usually evaluated by using bottle test and TGA test methods. In bottle test, particles are dispersed into brine and sealed in bottle, during which oxygen is supposed to be removed in the dispersion. To simulate reservoir temperature, the bottles are put into ovens and aged. At given intervals of period, dispersion in the bottles can be taken out for viscosity and particle size measurement. The alternation of viscosity and morphology can reveal the thermal stability change of particles [9,16,31,81,82].

Thermogravimetric analysis (TGA) is also used for thermal stability test. TGA can provide results of mass variations before and after being heated to an increasing temperature [26,36,41]. The temperature resistance from TGA is usually higher than bottle test because hydrolysis in aqueous condition is not considered in TGA. Salunkhe et al. performed TGA analysis of swollen particle gels at freeze-dried status with different aging time, the results showed there was not obvious change of TGA curves, which revealed no composition change during the thermal stability test [83]. However, bottle test should be more accurate than TGA because it includes hydrolysis of polymer.

5. Injectivity and transport

Transporting to desirable region/location is an essential requirement for micro/nanogel field application. The transport of microgel in porous media can be divided into six patterns, including direct pass, adsorption and retention, deform and pass, snap-off and pass, shrink and pass, and trap [40–44], which is controlled by the ratio of swollen particle diameter to pore diameter, particle strength, concentration, interaction forces and the driving force. In terms of nanogels, motion, retention and blocking are the main transport behaviors [12,54,84], and factors that influence the transport of nanogels are almost same with microgels [85]. The focus of the work is on particles smaller than 10 μm.

Transport of micro/nanogels can be divided into two categories: transport in single water phase and multiple phases. Many experimental studies have been conducted to investigate the transport of micro/nanogels in porous media, which includes core flooding test using sandpack and consolidate cores, filtration test and microfluidic model. Coreflooding test is the most common experiment to study particles transport through porous media, the experiment setup of which consists of sandpack/coreholder, pressure detection system, accumulator, pump and temperature controlling system. In the experiments, particles dispersed in brine are injected into sandpack/core with single phase or multiple phases, and the experiments can study the influence of flow rate, particle concentration, particle size and permeability. The recorded data include pressure at different point, effluent concentration of particles and oil production etc. Using the results generates resistance factor, residual resistance factor, plugging efficiency, matching factors, adsorbed layer, retention capacity and breakthrough time.

5.1. Injectivity evaluation

Micro/nanogel dispersion can be prepared by either dry powder or original emulsion, which should be consistent with the applications in oilfields. After obtaining the dispersion, some researchers injected dispersion with fully swollen particle [12,37,57,85,86], while others injected particles without swelling [10,58,87–89], depending on the swelling rate of the particles used in experiments. For fast-swelling rate particles, it would be better to have swollen particles to evaluate injectivity because these particles have swelled a lot in mixing and wellbore before entering the reservoirs. For slow-swelling rate or swelling delayed particles, different swelling time/ratio should be considered to evaluate the injectivity at different stages, which is trying to simulate particle size in different transport stages. Table 4 is an

Table 4
Experimental studies of micro/nanogel injection.

Researchers	Powder/ Emulsion	Swollen/ Initial size	Multiphase/ water phase	PV	Pressure measurement
Zhao et al. [49]	Powder	Initial size	Water phase	6–12.5	Single point
Liu et al. [65]	Emulsion	Injection at initial size, swelling in cores	Water phase	5	Multipoint
Yuan et al. [86]	Powder	Swollen size	Water phase	1.5	Single point
Sun et al. [58]	Powder	Initial size	Water phase	5	Single point
Ding[85]	Powder	Swollen size	Multiphase	15	Single point
Geng et al. [12]	Powder	Swollen size	Multiphase	1.5	Single point
Cao et al. [90]	Emulsion	Initial size	Multiphase	8	Single point
Yu et al. [37]	Powder	Swollen size	Water phase	10	Single point
Li et al.[57]	Powder	Swollen size	Water phase	2	Single point
Shi et al. [88]	Powder	Initial size	Multiphase	1–1.5	Single point
Li et al.[43]	Powder	Initial size	Water phase	4–6	Single point
He et al. [10]	Powder	Initial size	Water phase	1	Single point
Nie et al. [89]	Emulsion	Initial size	Water phase	1	Single point
Liu et al. [27]	Powder	Swollen size	Water phase	1.5	Single point
Jin et al. [59]	Emulsion	Swollen size	Multiphase	2	Multipoint
Chen et al. [45]	Powder	Swollen size	Water phase	3.8	Multipoint
Zhang et al. [34]	Powder	Swollen size	Water phase	5.8	Single point
Zhao et al. [66]	Powder	Initial size and swollen size	Water phase	0.3–0.5	Single point

Powder/Emulsion: When the researchers dispersed micro/nanogel, the status of particle is powder or emulsion.
Swollen/Initial size: When the researchers injected micro/nanogel, the particle is injected after swelling or not.
Multiphase/water phase: Multiphase is existence of oil phase and water phase.
PV: Injection volume measured by the unit of pore volume.
Pressure measurement: Single point means only one pressure sensor, and pressure curves reach to stable. Multipoint means more than one pressure sensor along the model, and pressure increase at all the points.

experimental summary of the micro/nanogel coreflooding tests, including dispersion preparation methods, particle swelling or not, multiphase or single water phase, injection volume and pressure measurement.

Moreover, the existence of oil saturation should be considered in coreflooding tests. Most of experiments are performed in single water phase [10,37,43,49,57,58,65,86]. In the experiments of multiphase, they are mainly conducted to show the oil recovery capacity. But we can still focus on their injection pressure in these multiphase experiments. Basically, micro/nanogels were injected when oil saturation was already decreased by waterflooding, and pressure was recorded at the same time [37,63,90]. It can be seen that the injection pressure in multiphase is higher than the one in single phase [12,85,88] because water relative permeability is lower in multiphase. Besides, it is observed that particle injection pressure start to increase after waterflooding [59,62,91], and the injection process is accompanied with decrease of oil saturation in cores, resulting in an increase of water relative permeability. Thus, these experiments cannot investigate an injection pressure at a constant oil/water saturation, which makes difficult to study the effect of oil on particle transport.

In Table 4, most of researchers used more than 1 PV to run the experiments [34,43,49,65,90]. In fact, it is hard to reflect injection ability of particles if injection volume is not more than 1PV. On one hand, the pore space has not been filled with particle suspension entirely as shown in the Fig. 12. On the other hand, if a core is taken from near wellbore area, more than 1 PV of particle suspension would transport through the pore space in the core. So, particle dispersion should be injected until the pressure is stable to reach steady state flow condition, at which condition the injection volume is usually larger than 1PV to test injection ability.

In terms of pressure measurement, most experiments utilized single pressure sensor. With single pressure curve, Yao and Wu et al. divided injection pressure curves into three types including destructive plug, effective plug and ineffective plug [5,13]. According to their dividing methods, destructive plug (severe surface plugging could be a better description) has a sharply increasing injection pressure, but its post waterflooding pressure is very low because the particles are too large to enter the cores. For ineffective plug, both injection pressure and post waterflooding pressure are very low because most particles flow through the cores directly. For effective plug, there is an increasing injection pressure and a relatively high subsequent waterflooding pressure, which is regarded as a good matched with porous media as shown in Fig. 13. In fact, the continually increasing pressure reflects an unstable flow status, indicating the particle retention does not reach the maximum value and the permeability will keep decreasing if particles are continuously injected. Although they suggested that the red curve in Fig. 13 is destructive plug/severe surface plugging, the maintained pressure of subsequent waterflooding (effective plug in purple, green and blue of Fig. 13) cannot be regarded as good transport in the cores. The reason is that these plugging may be formed at several centimeters deep of cores, leaving the majority of the remaining part undisturbed, which can be seen very clearly in the experiments with multipoint pressure sensors.

For example, Yang et al. also injected microgel in a 100 cm-long sandpack, the pressure sensor at inlet increased to 0.25 MPa at 8 PV, but the pressure sensor C and D stayed very low at 8PV as shown in Fig. 14,

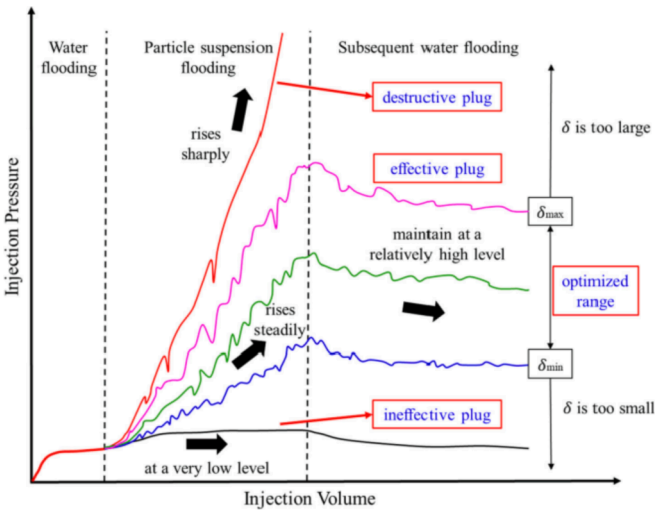

Fig. 13. Injection pressures curves with different particle size [5].

which means the overall injection pressure was contributed by plugging at the front of sandpack [92]. It also needs to be mentioned that the subsequent waterflooding provided lower pressure difference along cores and sandpacks than particle injection. Thus, if a severe plugging occurs, it is less possible to move the all the plugged particles during the subsequent waterflooding. Therefore, the plugging efficiency of single pressure curve is not a good indicator to transport.

If we focus on injection pressure curve without considering plugging efficiency, Cao et al divided injection pressure into plugging, passing through in deformation or broken status, deep migration by the slope of fitted pressure curves [86]. Yang et al. compared injection pressure by different particle size, and they proposed migration, blockage and seepage curves [92].

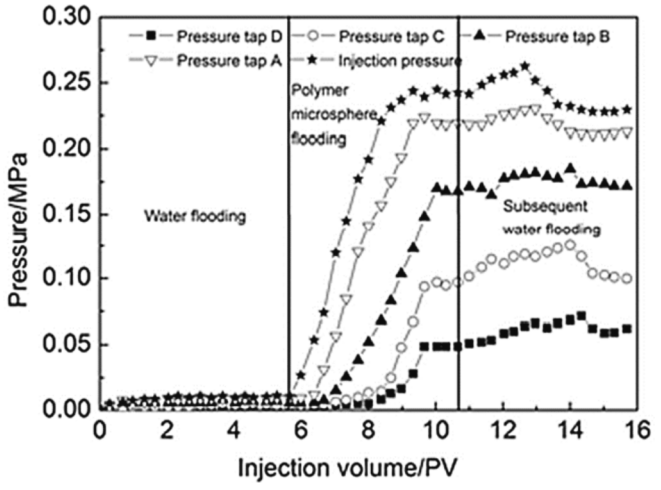

Fig. 14. Injection pressures curves with multiple pressure sensors [92].

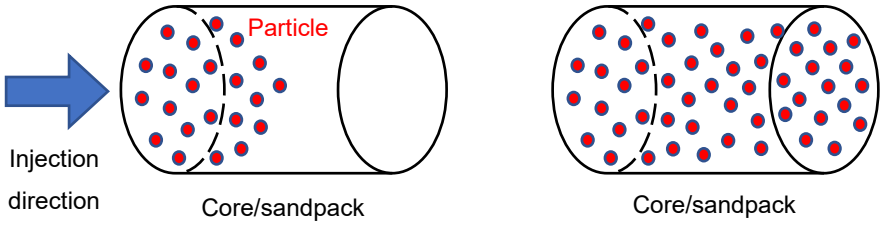

Fig. 12. Comparison between 0.5PV injection and 1 PV injection.

In our perspectives, the injection pressure curve should be flat and stable if single pressure sensor is used because it can make sure the particles transport without plugging at the front of cores. As shown in Fig. 15, we believe that the blue curve represents good injectivity, and the green curve also represents transport with deformation. The fluctuation of pressure curves usually means that the particle deform and pass through pore throats [56,59,92,93]. The overall trend of red and yellow curves is increasing, and they should not be regarded as good injectivity in our opinions.

The other experiments are carried out with multipoint pressure sensors [45,59,65,94]. Since increasing pressure at a certain pressure sensor might be viewed as particle arrival, pressure curves from multipoint pressure sensors are more convincing for injectivity. Similarly, stable pressure curves in multipoint pressure experiments are also preferred due to a balance between transport and retention of particles. If the injection pressure keeps increasing, it would be harder and harder to inject particles. For example, Li et al. built an 18 m-long model to evaluate injection and transport of microgel. With pressure gradient of 6.14 psi/ft, the particles only transported 10 m in the model when 4–5 PV of microgel was injected [95]. It is a typical particle transport issue in the depth of reservoirs, which is discussed in the following.

5.2. Particle transport issue

This is a very important issue that should be carefully considered in experimental design. However, most experimental designs do not have such a consideration, their pressure gradients in coreflooding experiments are too high to represent in-depth transport condition. The pressure gradients of some experiments are collected as shown in Table 5. What's more, Table 5 is a summary of experimental results that can be regarded as effective transport according to the following reasons: 1) The injection pressure is stable; 2) Or the pressure curve fluctuates up and down over 1 PV; 3) For multipoint pressure curve, all the pressure curves should increase during the injection. We believe the particles really transported through porous media in these experiments. The pressure gradient is calculated in the table by dividing the stable injection pressure (psi) by the length of porous media (ft). Yao et al. defined matching factor using average particle diameter divided by average pore diameter [13]. Sun et al. considered the distribution of particle size and pore size and defined matching factor at D10 D30 D70 and D90 [58]. Here we adopt Yao's definition, and the average pore size D can be calculated by the following equation:

$$D = \sqrt{\frac{8K}{\phi}}$$

where K and ϕ is permeability (μm^2) and porosity (%), respectively. Then matching factor$M$can be calculated as:

$$M = \frac{d}{D}$$

where d and D is mean particle diameter (μm) and average pore size (μm) of porous media, respectively.

According to Table 5 and Fig. 16, all the pressure gradients are higher than 1 psi/ft, and most of them are higher than 10 psi/ft. But the pressure gradients cannot represent real transport pressure gradient in the depth of reservoirs, due to the following reasons.

Although pressure gradient is quite high in near wellbore area, the situation in the depth of reservoirs is different. Here is an example of pressure gradient in a 2D radical flow pattern as shown in Fig. 17. It is assumed that injection pressure of an injection well ranges from 5000 to 2000 psi. The boundary pressure is 1000 psi around the injection well. The radius of injection wellbore and boundary is 0.3ft and 1000ft, respectively. Then, we can have a pressure gradient calculation as following:

$$\frac{dP}{dr} = \frac{P_{wf} - P_e}{\ln \frac{r_w}{r_e}} \times \frac{1}{r}$$

where $\frac{dP}{dr}$ is pressure gradient, $P_{wf}$and P_e are injection pressure and boundary pressure in psi, respectively, r_w,r_e and r are wellbore radius, boundary radius and distance in ft, respectively. The calculation results are shown in Fig. 17.

According to the calculation results, when the injection pressure ranges from 2000 psi to 5000 psi, the pressure gradient is lower than 1 psi/ft at 500 ft away from wellbore, and most of pressure difference is distributed near wellbore. Besides, there are not any parameters related with permeability or viscosity in the calculation, which means the low-pressure gradient exists in a variety of reservoirs. Therefore, whether particle transport at such a low-pressure gradient is questionable because most of the coreflooding tests were not well designed to reflect the real pressure gradient in the in-depth of reservoirs.

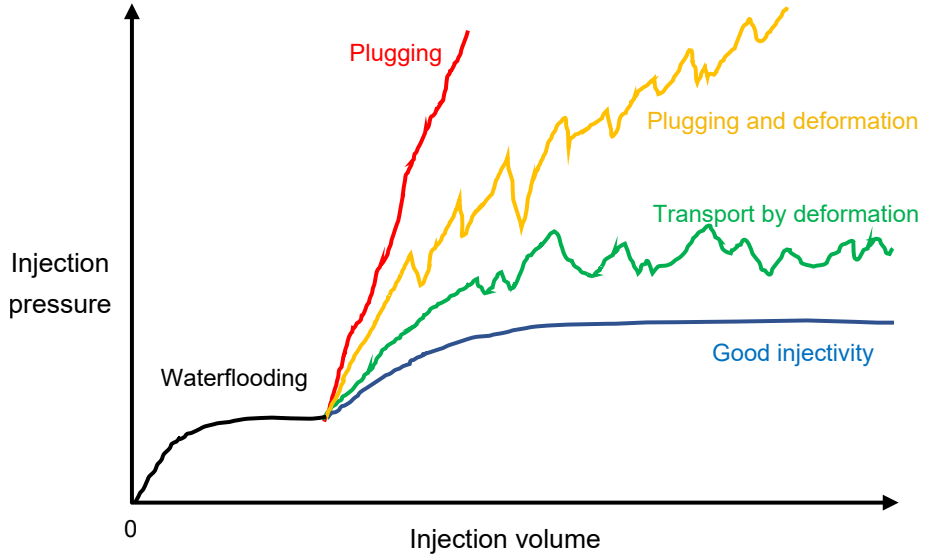

Fig. 15. Injection pressures curves of single pressure sensor.

Table 5
Summary of effective transport experiments.

Researchers	Flow rate/(mL/min)	Concentration/(w.t.%)	Matching factor	Pressure gradient/(psi/ft)
Zhao et al. [49]	0.5	0.5	0.586	5.89
	0.5	0.5	0.799	12.38
	0.5	0.5	1.016	27.11
	0.5	0.5	1.143	80.16
	0.5	0.5	1.203	123.78
	0.5	0.5	1.550	337.16
	0.5	0.5	1.693	531.67
	0.5	0.5	1.988	890.04
Liu et al.[65]	0.9	0.3	1.252	48.63
Yuan et al. [86]	0.5	0.1	1.013	70.73
	0.5	0.1	0.853	64.84
	0.5	0.1	0.746	29.47
Sun et al. [58,60]	0.5	0.3	1.020	312.32
	0.5	0.3	0.600	52.38
	0.5	0.3	0.480	26.51
	0.5	0.3	1.450	595.06
	0.5	0.3	1.200	396.98
	0.5	0.3	0.900	176.98
	0.5	0.3	0.640	107.30
	0.5	0.3	0.510	40.27
Ding[85]	0.5	0.1	0.048	21.34
	1.25	0.1	0.043	35.36
	3	0.1	0.043	91.44
	0.5	0.1	0.024	30.04
	0.5	0.1	0.017	10.89
	0.5	0.1	0.012	2.39
Geng et al. [12]	0.25	0.1	0.035	3.10
Cao et al.[90]	0.5	0.5	0.030	1.89
	0.5	0.5	0.007	2.87
	0.5	0.5	0.030	1.36
Yu et al.[37]	0.5	0.05	0.055	59.24
	0.5	0.05	0.048	57.47
Li et al.[57]	0.5	2	0.090	318.29
	0.5	2	0.112	583.54
Shi et al.[88]	0.5	0.1	0.345	60.96
	0.5	0.1	0.411	91.44
Li et al.[43]	0.3	0.3	1.129	110.52
	0.3	0.3	1.284	390.14
	0.3	0.3	1.333	79.57
	0.3	0.3	1.456	221.04
	0.3	0.3	1.299	110.52
	0.3	0.3	1.228	27.43
He et al.[10]	0.1	0.2	0.375	14.74
Nie et al.[89]	0.5	0.2	0.004	1.03
	0.5	0.2	0.005	4.42
	0.5	0.2	0.006	129.68
	0.5	0.2	0.017	1.47
	0.5	0.2	0.020	8.69
	0.5	0.2	0.025	29.47
	0.5	0.2	0.049	2.95
	0.5	0.2	0.059	16.95
	0.5	0.2	0.072	110.52
	0.5	0.2	0.212	9.14
	0.5	0.2	0.255	100.20
Jin et al.[59]	0.5	0.5	0.166	2.76
Chen et al. [45]	0.2	0.1	0.380	11.79
Zhang et al. [34]	0.34	0.15	0.124	18.79
	0.34	0.15	0.398	30.28
Zhao et al. [66]	0.3	0.3	0.095	42.00
	0.3	0.3	0.455	53.05
	0.3	0.3	0.622	55.26
	0.3	0.3	0.492	55.26
	0.3	0.3	1.417	42.00

5.3. Particle retention

While a stable injection pressure is a prerequisite for injection ability, relatively low retention is also an important requirement during micro/nanogel transport stage (However, retention is favorable for in-depth fluid diversion purpose). Retention of particles consists of physical plugging and adsorption (Fig. 18). Physical plugging includes mechanical trapping and log-jamming [75,96]. Log-jamming is the blockage of pores that are larger than each particle, which results from the accumulation of particles at the pore throat entrance due to different transport velocity between particles and fluid (Fig. 19). The main factors governing the log-jamming effect are particle concentration, effective hydrodynamic size, pore size distribution and flow rate [97]. Adsorption can be divided into irreversible adsorption and reversible adsorption. Reversible adsorption means particle can be removed in post water-flooding, whereas irreversible adsorption is permanent.

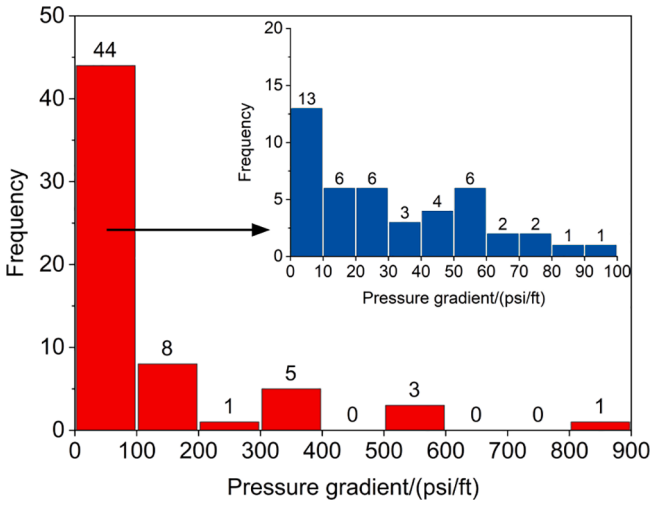

Fig. 16. Injection pressures gradient distribution.

Physical plugging is the main retention mechanism of particles which are close to or larger than pore throat. Many researchers, such as Yao et al. [93], Hua et al. [98] and Li et al. [99], have investigated it using transparent microfluidic models and microgel which can be observed easily by microscope. They classified the plugging into elastic plugging, bridge plugging and complete plugging, depending on particle size and elasticity [17,45,95,100]. Membrane filtration test is a simple method to evaluate plugging of particle suspension. The test can tell if the particle can block the membrane by the relationship between the filtration volume and the filtration time of suspension. The equilibrium filtration rate is an essential parameter to indicate the transport behavior during steady state [47]. Hua et al. conducted SEM and filtration tests to observe the plugging, and they suggested one third of pore size is an important parameter for plugging, which was also proposed in other microgel research [45,63,95,101]. However, traditional SEM need a dry sample, the original particle size had already shrunk before observation. The combination of E-SEM and filtration test could be better to observe the plugging with its original status.

In general, plugging efficiency and residual resistance factor are mainly influenced by particle size, injection rate, particle concentration and particle elasticity etc. in coreflooding test. Small size leads to less plugging and lower residual resistance factor [86,88,102]. However, it also causes surface plugging and results in low plugging efficiency if the particle is too large and it cannot enter the porous media [13]. High plugging efficiency can be achieved by low injection rate and high concentration [66,85,103]. In terms of elasticity, the situation is more complex. When the ratio of particle size to pore size is controlled, particles with high elasticity are more difficult to deform and transport. This phenomenon has been observed in many experiments, including nanogel, microgel and PPG [49,104–106]. Also, some numerical simulation studies show the similar results [56,107]. However, particle to pore size ratio is a more dominant parameter. When particle size is much smaller than pore size, elasticity is not that important [101]. When particle size is close to pore size, higher elasticity leads to higher injection pressure

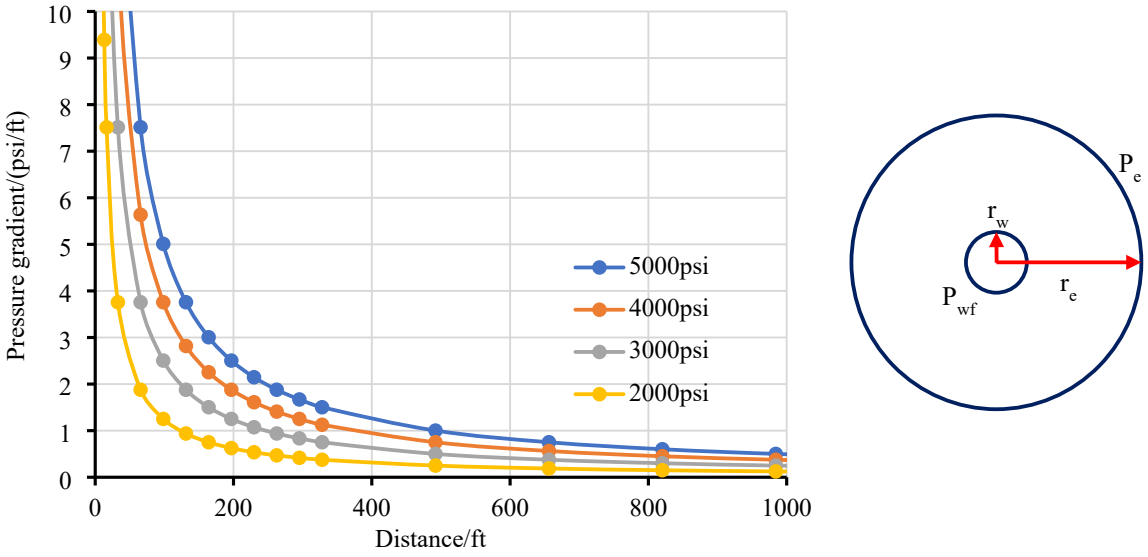

Fig. 17. Illustration of pressure gradient distribution.

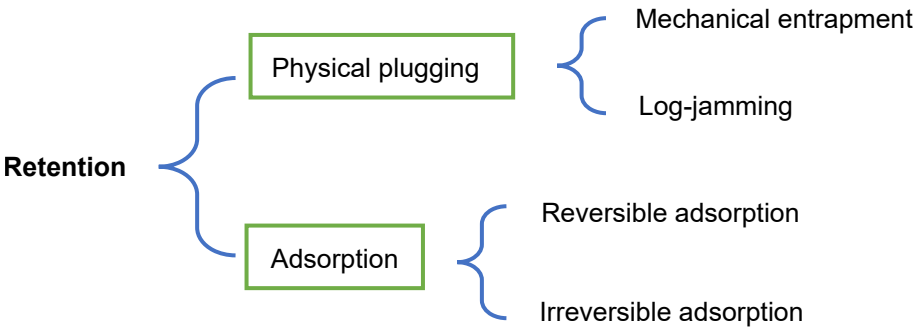

Fig. 18. Retention categories.

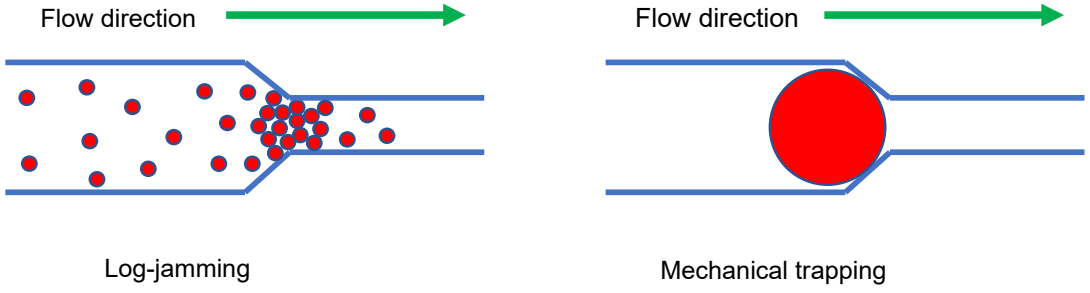

Fig. 19. Illustration of log-jamming and mechanical trapping.

and higher plugging efficiency [49].

Adsorption is a property of nanoparticles, and various types of nanoparticles show different adsorption properties [108]. McDowell-Boyer et al. proposed three kinds of filtration mechanisms of solid particles during transport in porous media: surface filtration, straining and physicochemical filtration [109]. Particle transport is determined by physicochemical filtration, which is the interactions between neighboring nanoparticles and between particles and porous medium surfaces [110]. Theoretically, polymeric nanogels should share some of these transport mechanisms, even though most nanogels published in oil recovery-related literatures have diameters of a few hundred nanometers, because they are all colloids and follow DLVO theory. However, the research of nanogel transport and adsorption in dynamic condition is bare. Only Geng et al. suggested a similar adsorption kinetics in interfacial tension reduction explanation [12]. But their adsorption kinetics is based on static adsorption. Overall, the transport process of nanogels could have two stages as shown in Fig. 20. The first is diffusion-controlled process in diffusion boundary layer. Diffusion boundary layer is defined as the near surface region in which colloid transport is dominated by diffusion. Second, colloid transport is controlled by advection of fluid beyond the diffusion boundary layer [111].

In retention experiments, sandpack is used to measure the retention amount in porous media, including three types of methods. The first one is utilizing mobility reduction and layer thickness by which the amount

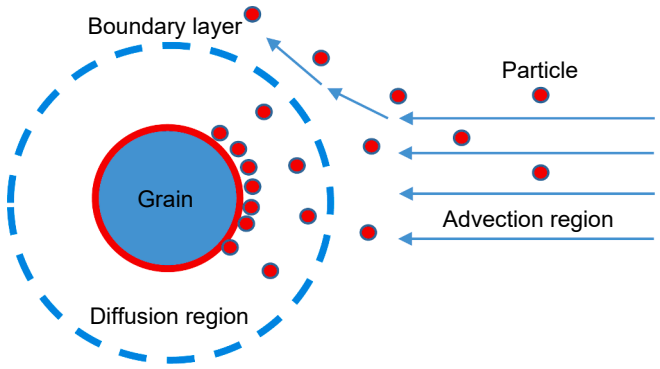

Fig. 20. Diffusion boundary layer.

of retention is calculated. For example, Chauveteau et al. investigated microgel propagation by multipoint pressure sensor on sandpack. The adsorbed layer thickness and adsorption distribution in each section of model were calculated by permeability reduction [81,82,112,113]. But the permeability reduction cannot distinguish the difference between mechanical trapping and adsorption. To observe the particle in porous media, some studies provided SEM photos for core cuttings in microscale [95,102]. However, the particles were already dried during the SEM preparation process, which cannot reflect the original status of particle distribution. The second method is using a specially designed sandpack model. In addition to multipoint pressure sensor on sandpack, this kind of sandpack can be divided into several parts and the component of each part can be analyzed using UV Visible Spectroscopy test. Thus, the concentration in different part of sandpack is measured, and transport of particle can be confirmed [114]. Although sandpack can show the concentration distribution of particles, the interference resulting from sand produces some errors in UV test. The third method, which is also the most common one, is analyzing concentration history of effluents by UV or Total Organic Analyzer (TOC) as shown in Fig. 21. In the experiment, NaCl or KCl solution is usually injected as a tracer which can be compared with particle suspension. The amount of adsorbed particle is calculated using cumulative mass balance. Yao et al. performed such experiments for microgel, and the retention results show that only 10 % of the injected particles were recovered in the effluent [100]. Zhang et al. and Yu applied the method for silica nanoparticles, and the results show that 80 %-90 % of nanoparticle can transport through their model [115,116]. The main difference could be due to the ratio of particle size to pore size and surface charge. Cao et al conducted retention tests by different particle size in carbonate, he found small particle may has high retention because of aggregation [90]. In terms of polymeric nanogels, Lenchenkov used TOC to measure polymer nanogel effluent concentration, and he found the producing concentration is only 10 % of injected concentration after 2 PV injection [117]. Geng et al. investigated surface charge effect on adsorption and adsorption kinetics, and he suggested positive nanogel had the higher adsorption in sandstone [12]. Currently, most of researchers only focus on transport in single water phase.

Here is summary for coreflooding experiments aiming to evaluate

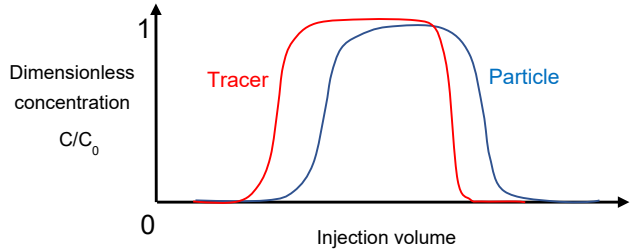

Fig. 21. An example of effluent history.

injectivity and transport. Pressure curves are indicators to show whether particle can be injected, and stable and flat pressure curves are preferred. However, this is only one prerequisite for transport. Retention experiment is also needed to illustrate migration ability. A good transport evaluation experiment should combine these two together.

In recent years, microfluidic model is being widely applied in oil & gas industry. Microfluidic model can show injection pressure and observe the transport of particle directly at the same time. Compared with the core-flooding experiments, microfluidic has significant advantages in visualization, controllability, and repeatability. But the disadvantages lay in the differences between real reservoir environment, such as temperature, pressure, clay and rock surface, and micromodel environment. Generally, micromodel can be divided into one dimension, two dimensions and three dimensions. One dimension model is usually a capillary tube which can be used to analyze the transport of singe particle [32,63,118]. Quantification of threshold pressure and injection pressure can be analyzed using this kind of model [99,107]. Besides, the model can quantitatively analyze retention patterns and flow resistance variation caused by different patterns [93]. Basically, one-dimension models are applied for injection pressure and elasticity investigation in single phase transport. Currently, most micromodels are two-dimension micromodels with random porous structures in only two-dimensional fluid channels. Bai et al. investigated the transport patterns and threshold pressure gradient using etched glass model [119]. The corresponding relationship of matching factors and passing through patterns in different storage modulus was established by Yang [92]. Pu et al. found that particle could re-migrate in the high permeability area and displace residual oil due to elastic deformation [61]. Cao et al. studied the effect of micromodel wettability for particle injection [87]. Chen at al simulated the deformation of microgel under compression with the data obtained from two-dimension models [120]. Compared with one dimension model, two dimensions model can explore multiphase effect, wettability effect and oil displacement capacity, not only injection pressure and elasticity. But the fabrication of two dimensions models is more complex and time consuming. Three dimensions micromodels are usually built by sintering silicate glass beads in a capillary tube to mimic the real connected porous media [121]. Yao et al. built a transparent sandpack micromodel that was used to observe the microscopic flow and displacement mechanisms [17]. Zhang et al. directly visualized the different size of microgel flow in three-dimensional micromodel [52]. Zhang et al. visualized the flow of nanogel in a transparent three-dimensional micromodel, and they discuss the emulsification ability of nanogel [67]. Microgels are easily observed in three-dimensional micromodel, but it is still difficult to observe nanogels in these experiments due to the small size.

6. EOR mechanisms

Microgel and nanogels are regarded as promising EOR agents and have been used in many oilfields, especially in China [4,62,66,103]. These polymeric particles have a controllable and smaller size compared with traditional preformed particle gel (PPG), and they can be designed to have good thermal stability. Although both microgel and nanogel pilot tests have shown water management and improved oil recovery [4,122,123], the EOR mechanisms of microgels and nanogels may be distinct.

Microgels:

It is widely reported that well-designed microgels can enter and plug the high permeable zone of reservoirs [7,11,62]. The main conformance control mechanism is to reduce the permeability of swept high permeable zones/areas, and unswept low permeable zones/areas should not be invaded and damaged. Some microgels with triggers can keep a relatively small size during injection and transport stages. When the surrounding environment changes, such as salinity, pH value, and temperature, repulsions among polymer chains in gel particles increase and particles can swell much larger than initial status [7,124,125]. Pu

et al. [61] and Chauveteau et al. [81] believe the microgel can reduce the permeability of water, and achieve disproportionate permeability reduction (DPR). Besides, studies have shown that microgel is able to block pores and then redistribute fluid flow on a microscopic level [8,27,120]. Splido et al. suggested microgel can improve microscopic sweep efficiency by redistribution of flow at microscopic level [125]. Pu et al. measured relative permeability and they found the decreased residual oil saturation after microgel injection [61]. Some researchers combined NMR with coreflooding tests to demonstrate sweep efficiency improvement at pore scale by the alteration of oil saturation during the flooding [126–128].

When particle size becomes smaller, the interfacial energy increases a lot, and particles present a number of favorable characteristics, such as high specific surface area and special chemical responses. Even microgel in 1 or 2 μm, it can also adsorb at interface and form Pickering emulsion as shown in Fig. 22 [129].

Nanogels:

Nanogels are significantly smaller and have a larger surface area than microgels, allowing them to have features that microgels do not. Currently, the EOR mechanisms of nanogels are not very clear [104,130,131]. However, many studies have been conducted on the EOR mechanisms of nanoparticles, and we will show and discuss the potential mechanisms in the follow.

6.1. Spreading mechanism

Spreading and disjoin pressure are one of EOR mechanisms for nanoparticles. The nanoparticles in dispersion can form a self-assembled wedge-shaped film at the three phases contact, and this wedge film acts to separate fluids (disjoining pressure), such as oil, water and gas, from the solid surface [75,132–139]. This arrangement of nanoparticles and its spreading force exert additional pressure at that interface, which is higher than the pressure in the bulk fluid. Thus, driven by this pressure, the nanoparticles tend to spread along the surface. Disjoining pressure of the film can be expressed as the sum of van der Waals' force, electrostatic force and structural force [140]. Trokhymchuk et al. gave an analytical expression for disjoining pressure [133]:

$\Pi(h) = \Pi_0 \cos(\omega h + \phi_2) e^{-\kappa h} + \Pi_1 e^{-\delta(h-d)}$ for $h \geq d$,

$\Pi(h) = -P$ for $0 < h < d$. where $\Pi(h)$ is disjoining pressure, d is the diameter of particle, h is the film thickness, P is the bulk osmotic pressure from nanoparticles, $\Pi_0, \Pi_1, \phi_2, \omega, \kappa, \delta$ are fitted as cubic polynomials in terms of particle volume fraction.

This mechanism aims to explain movement of oil which is attached on the rock surface as shown in Fig. 23, and Table 6 is a summary of spreading studies. To our best knowledge, there is not any experimental studies or modeling studies of spreading mechanism of polymeric nanogel.

According to these studies, spreading is promoted by small particle size, low polydispersity, low equilibrium contact angle, and high concentration [134,144]. However, the disjoining of oil drop not only need spreading, but also disjoining pressure to remove oil drop. Although spreading phenomenon has been directly observed, aggregation of particles, reservoir environment and dynamic condition are not considered. What's more, whether nanogel exhibits such a disjoining pressure is still unknown because the swollen nanogels are usually a few hundred nanometers, which are much larger than the traditional nanoparticles above. Therefore, the disjoining pressure may not be very high, and experiments and modeling are needed to estimate disjoining pressure and film energy for nanogels.

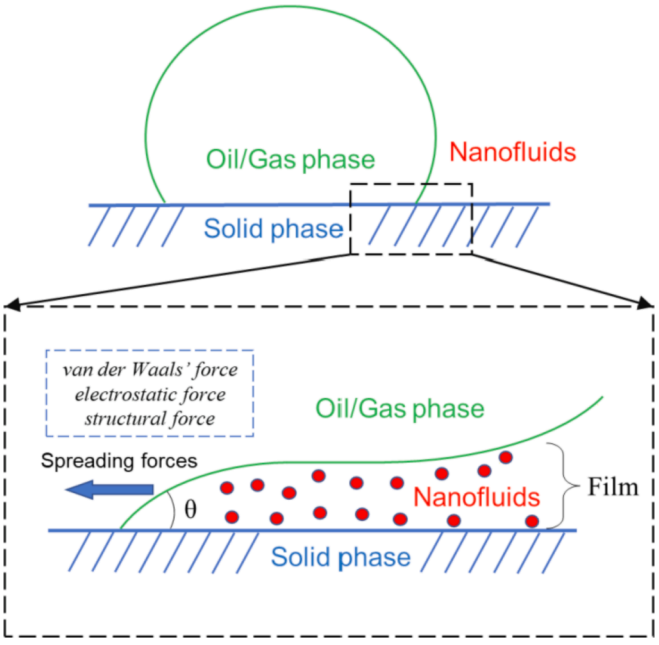

Fig. 23. Spreading forces profile.

6.2. Interfacial tension reduction and wettability alternation mechanism

Interfacial tension reduction and wettability alternation also contribute to EOR. These two phenomena are owed to nanogel adsorption at the interface, which shows a very similar behavior with surfactants. It is believed that this phenomenon occurs because the adsorption lowers the total system energy. However, there is a long ongoing debate on whether nanoparticles can enhance oil recovery by the reduction of interfacial tension and wettability alternation [145]. Nanogels can reduce interfacial tension by adsorption at the interface [85,91,146] and forming Pickering emulsion [67]. But the reduction degree is not much compared with surfactants. With existence of particles, interfacial tension may decrease to a few mN/m. However, the interfacial tension can

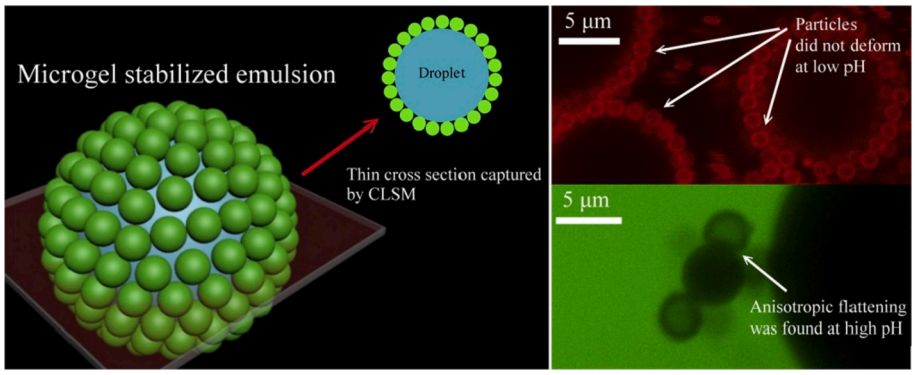

Fig. 22. Pickering emulsion formed by microgel with 1.7 μm [129].

Table 6
Briefly summary of spreading phenomena.

Researchers	Nanoparticles	Size	Summary of major findings	Disjoining pressure
Wasan et al. [132]	Latex particles	8 nm	Calculated the pressure arising at wedge vertex. Demonstrate the crystal-like ordering of nanoparticle in water.	50 KPa
Chengara et al.[133]	General nanoparticles	20 nm	Using Laplace equation, examined the effects of nanoparticle size, concentration and polydispersity on the displacement of an oil–aqueous interface.	More than 20 KPa
Sefiane et al. [140]	Aluminum nanoparticles	40–120 nm	Enhanced dynamic wetting behavior of nanofluids was experimentally evidenced.	N/A
Liu et al. [136]	SiO_2	20–30 nm	Spreading process is modeled by Navier–Stokes equations, which considers the structural disjoining pressure, gravity, and van der Waals force.	3.3 KPa
Zhang et al. [138]	SiO_2	20 nm	Presents the results of imbibition tests using a reservoir crude oil and a reservoir brine solution with a high salinity and a suitable nanofluid that displaces crude oil from Berea sandstone	100 KPa
Moghaddam et al.[139]	ZrO_2, $CaCO_3$ TiO_2, SiO_2 MgO, Al_2O_3 CeO_2	35–40 nm	Disjoining pressure was the responsible mechanism for changing dynamic wettability and remove oil from the surface	More than 48 KPa
Sharma et al. [141]	SiO_2	15 nm	Stability and viscosity of nanofluids, the efficiency for EOR is a function of temperature.	N/A
Kuang et al. [142]	Al_2O_3 SiO_2 TiO_2	10–50 nm	Investigate synergistic effects of nanofluids on interfacial properties of oil/ brine/rock systems and their role in influencing oil displacement from sandstone and carbonate rock.	N/A
Zhao et al. [143]	Silica nanoparticles	15–30 nm	Better EOR ability than surfactants in imbibition due to disjoining pressure.	N/A
Kondiparty et al.[144]	Silica nanoparticles	20 nm	A nanofluid with an effective particle size, a low equilibrium contact angle, and a high concentration, are desirable for the dynamic spreading of a nanofluid system.	8–2110 KPa

decrease several magnitudes when surfactants are added [46]. What's more, despite some researchers suggested capillary number increase [147], the increase of capillary number by adding nanoparticle is not large enough to reduce residual oil saturation [97]. The regular definition of capillary number, without considering wettability, is:

$$N_c = \frac{\nu\mu}{\sigma}$$

where $\nu$and $\mu$are velocity and viscosity, respectively. The viscosity improvement by nanoparticle is not much [141,148]. If σ decrease 90 %, the capillary number will only increase 10 times (Fig. 24). In the Table 7, most of the interfacial reduction even cannot decrease 90 %. Thus, the increase of capillary number does not account for the residual oil saturation reduction. There are other capillary numbers that consist of contact angle, such as$N_c^{'} = \frac{\nu\mu}{\sigma\cos\theta}$. But the capillary number could be infinite once contact angle is 90°. In addition, increase of capillary number is responsible for trapped oil in a capillary tube, rather than oil attached on the rock surface. Overall, residual oil saturation reduction is difficult to be explained by interfacial tension reduction only.

Wettability alternation is also regarded as a EOR mechanism for nanogels. Many studies have reported the application of nanoparticles in EOR through wettability alteration and contact angle change is also recorded as shown in Table 7. But studies of the polymeric nanogels are still rare. In general, contact angle measurement, imbibition test, permeability test and SEM are used to study wettability alternation. The contact angle measurements are conducted using static fluids, and most of them are performed at room temperature and atmosphere pressure [140,143,149,150]. Also, the measurement needs a very clean and even surface of the substrates, which is difficult to achieve. Imbibition test is another static experiment to show wettability alternation. Compared with brine imbibition, nanofluids have a better performance in oil recovery [138,139,143]. Kuang et al. characterized adsorption by Quartz Crystal Microbalance with Dissipation (QCM-D) instrument coupled with flow cells to monitor the real-time process [142]. In their SEM observation, the surface of adsorption was not evenly, and a very complex structure consisting of aggregations were found. In addition, relative permeability curves obtained by coreflooding tests have also shown the wettability alternation indirectly. It was observed that, after nanofluids injection, the relative permeability curves of cores moved to right [141,151], which means residual oil saturation was reduced and the porous media became more water wet. Pu et al. investigated the effect of

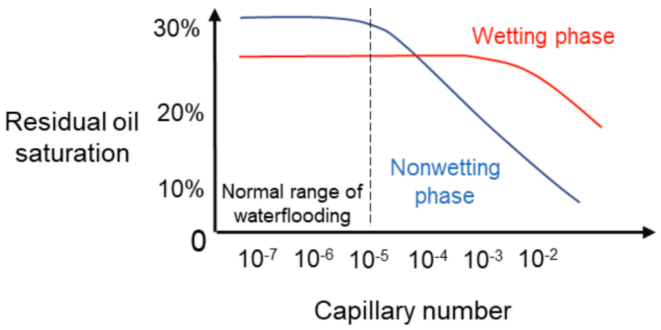

Fig. 24. Residual oil saturation and capillary number.

Table 7
Briefly summary of interfacial tension and contact angle reduction.

Researchers	Nanoparticles	Size/nm	Phase	Interfacial reduction	Contact angle alternation (degree)
Khellil Sefiane[140]	Aluminum nanoparticles	40–120	Air/water/ Silicon substrates	22 to 21mN/m	64° to 62°
Hendraningrat, Luky[149]	SiO_2	21–40	Crude oil /brine/silicon substrates	19.2 to 7.9mN/m	54° to 22°
Hua Zhang[138]	SiO_2	20	Decane/brine/ sandstone	16 to 1.4mN/m	74° to 1.2°
Nazari Moghaddam[139]	$CaCO_3$	35–40	Decane/brine/ carbonate	N/A	158° to 120°
Wendi Kuang[142]	Al_2O_3 SiO_2 TiO_2	10–50	Decane/brine/ sandstone	53 to 47mN/m	N/A
Mingwei Zhao[143]	Silica nanoparticles	15–30	Crude oil/ brine/glass	N/A	135° to 45°
Rezaei Amin [150]	SiO_2	18–38	Crude oil/ brine/rock	36.9 to 8.3mN/m	115° to 100°
B. Moradi[152]	SiO_2	11–14	Crude oil/ water/carbonate	13.6 to 10.7mN/m	122° to 16°
Jiaming Geng[12,146]	Nanogel	100–400	Decane/brine/ sandstone	26 to 4mN/m	23.6° to 15.5°

microgel concentration on the curves, and they suggested high concentration resulted in lower residual oil saturation and the curves moved to right more [61].

6.3. Sweep efficiency improvement mechanism

Nanogels can increase oil recovery by improving sweep efficiency, which shows a similar mechanism with microgels. When nanofluids flow through porous medium, log-jamming, mechanical entrapment and adsorption will result in plugging of the pores, then improved the sweep efficiency [137,149,153]. Compared with the first two mechanisms, sweep efficiency improvement could be the most important EOR mechanism because the size of nanogel is larger than conventional nanoparticles (silica). Table 8 is a summary of resistance factors and residual resistance factors of nanogels from Table 5 (effective transport). Although many researches, including coreflooding tests and micromodel experiments, have shown the plugging efficiency and enhanced oil recovery [137,148,154,155], the particles may be too small to improve sweep efficiency [97]. It can be seen that some of the residual resistance factors in Table 8 are not very high, which means these nanogels hardly improve sweep efficiency. It seems contradictory to have a good transport (small size) in injection and good retention (large size) in desirable location/region at same time, but it is also the key for application of micro/nanogels. A small size in transport and a large size in plugging or re-crosslinking are the ideal condition for EOR as we mentioned in the end of transport issue. This could be an advantage of polymeric nanogels, since conventional nanoparticles, such as SiO_2, do not have a swelling capacity. But how to control the swelling is another important issue. Zheng et al. synthesized swelling-delayed nanogel, and it took 30 days to fully swell [52]. Liu et al. proposed a re-crosslinking microgel which can form weak bulk gel [35].

Table 8
Summary of resistance factors and residual resistance factors.

Researchers	Particle size/nm	Permeability/ mD	Resistance factor	Residual resistance factor
Ding[85]	175	123	7.25	4.6
		125	4.9	2.5
		114	3.5	2.35
		114	2.85	2.4
		137	3	2.2
Yu et al.[37]	555	500	6.7	16.5
	482	500	7.2	21.7
Li et al.[57]	192	28	2.69	2.31
	266	34	5	3.85
Li et al.[43]	455	22.9	8.8	8.9
		17.2	25.5	26.4
	255	85.7	20.2	20.7
		70.5	54.8	57.4
	17	151.6	54.1	57.9
		177.5	15.7	16.2
Nie et al. [89]	47	1387	1.74	42.67
	47	769	2.7	63.03
	47	354	2.99	66.52
	209	1387	3.05	67.17
	209	769	4.51	77.63
	209	354	5.53	81.91
	611	1387	6.26	84.01
	611	769	10.12	90.12
	611	354	16.42	93.91
Liu et al.[27]	600	13.71	4.8	16.32
Almohsin [104]	158	143	10.5–12	10.5–12.5
	265		8–11.5	6.5–11.5
	285		6.8–11.2	5.5–10.5

Other mechanisms, such as viscosity enhancement of injection fluid, are mentioned in some publications [75,156]. But these mechanisms are not widely reported, and the viscosity enhancement is limited [148].

In summary, nanogels do have IFT reduction and wettability alternation ability according to the studies. However, since nanogel size is larger than normal nanoparticles, it is still unclear that how much these two mechanisms contribute to oil recovery (Fig. 25). With well-designed size, both microgels and nanogels could provide sweep efficiency improvement.

7. Current challenges and future research directions

Based on the review above, the experimental studies of micro/nanogels have been conducted by many researchers. But it is very clear that there are many key issues to be solved for a better application in oilfields.

1) It is difficult to directly measure particle mechanical strength. The bulk gel method and shearing method can only reflect particle mechanical strength indirectly. AFM method and micro/nanomanipulation method are limited by debatable theoretical models to explain the data. Besides, the selection of probe type of AFM is also questionable.
2) Injectivity evaluation is not well-designed in many coreflooding tests. Most of reported research results do not have a stable injection pressure in their experiments. Besides, these coreflooding tests were not well-designed to reflect the real pressure gradients in the in-depth of reservoirs.
3) Particle retention of nanogels lacks investigation. Polymeric nanogels should share some of adsorption mechanism of common nanoparticles, but the nanogels used in oilfields have larger diameters than conventional nanoparticles. Although there are many theories and experiments regarding to nanoparticles, there is no quantitative evaluation about nanogel transport and adsorption in dynamic conditions.
4) The mechanisms of nanogel EOR are unclear. No experimental studies or modeling studies of polymeric nanogels have been

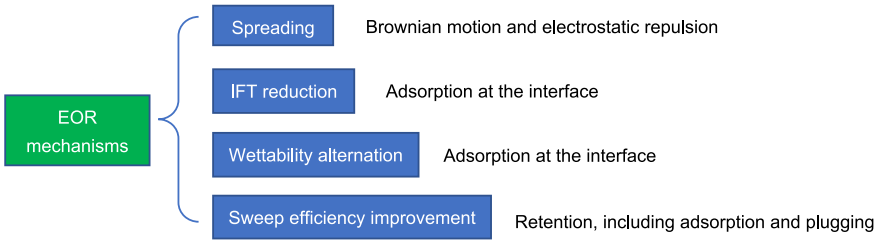

Fig. 25. Summary of nanogel EOR mechanisms.

reported regarding to whether spreading mechanism could be one major mechanism. Besides, interfacial tension reduction and capillary number increase caused by nanogels are limited and are not convincible to explain residual oil saturation reduction. The residual resistance factors for nanogels are usually too low to improve sweep efficiency.

5) It is important to have a nanogel that have a good transport ability (small size) during its movement to the in-depth and good retention (large size) after being placed. However, no such good robust nanogels are available at current market. Swelling delayed particles usually can control particle size but they become weak in strength after further swelling.

Based on the review, we recommend the following research directions that should be addressed to make the micro/nanogel technologies feasible for enhanced oil projects.

1) Methods to characterize micro-/nano-gel should be improved. Current methods to evaluate particle size and strength are not very reliable.
2) Novel micro/nanogels should be developed. re-crosslinkable micro/nanogels could have great potential to be applied but require them to have controllable re-crosslinking time and to be re-crosslinked at low concentrations. In addition, high temperature high salinity resistant micro/nanogels should be developed for harsh reservoir conditions.
3) Micro/nanogel injectivity, transport and plugging performance should be characterized to understand where microgels/nanogels can be best applied. Injection pressure or injection rate should be designed to reflect the practical pressure gradients available in reservoir during particle transport into the in-depth. Resistant factor, retention and plugging efficiency should be quantified considering multiple influencing factors such as particle size, concentration, strength, velocity, rock permeability, fluid saturation and so on.
4) EOR mechanisms should be further evaluated. Lab experiments need be better designed to investigate how the nanogel can improve oil recovery and whether the mechanisms can provide a key role in field applications. Numerical simulation method should be developed. After obtaining quantitively evaluation results of particle transport and plugging, it is necessary to develop mathematical models and numerical simulation method that can be used for optimizing micro/nanogel conformance control treatments.

8. Summary

This study reviewed the experimental evaluation methods and corresponding results of polymer micro/nanogels for EOR and reduced water production. From synthesis of micro/nanogels to evaluation of particles, we reviewed the experiments regarding to compositions, morphology, size determination, mechanical properties, stability of dispersion and thermal stability of micro/nanogels. When it comes to injectivity and transport, we suggested how to conduct micro/nanogel coreflooding test properly and found that injectivity evaluations were not well-designed in many coreflooding tests. In terms of EOR mechanisms, we critically discussed the spreading mechanism, interfacial tension reduction and wettability alternation, and sweep efficiency improvement mechanisms and concluded the EOR mechanisms of nanogel were unclear. Finally, we proposed the current challenges and future research directions based on the review.

Declaration of Competing Interest

The authors declare the following financial interests/personal relationships which may be considered as potential competing interests: Baojun Bai reports financial support was provided by Qatar National Research Fund.

Acknowledgment

The authors would like to acknowledge the Qatar National Research Fund (a member of Qatar Foundation) for funding through Grant # NPRP13S-1231-190009.

References

[1] Bai B, Huang F, Liu Y, Seright RS, Wang Y. Case study on preformed particle gel for in-depth fluid diversion. Proc - SPE Symp Improv Oil Recover 2008;3:1438–55. https://doi.org/10.2118/113997-ms.
[2] Hill F, Monroe S, Mohanan R. Water management - An increasing trend in the oil and gas industry. Soc Pet Eng - SPE/EAGE Eur Unconv Resour Conf Exhib 2012;2012:918–22. https://doi.org/10.2118/154720-ms.
[3] Bill B, Jeb T, Jon E, Fikri K. Water control Oilf Rev 2000;12:30–51.
[4] Hou G, Yuan X, Han P, Lu F, Jiao Z, Diwu P, et al. Field application of nano polymer microspheres profile control: A pilot test in ultra-low permeability oil reservoir. Soc Pet Eng - SPE Asia Pacific Oil Gas Conf Exhib 2020, APOG 2020 2020:1–14. https://doi.org/10.2118/202412-ms.
[5] Wu D, Zhou K, Hou J, An Z, Zhai M, Liu W. Review of experimental and simulation studies of enhanced oil recovery using viscoelastic particles. J Dispers Sci Technol 2021;42(7):956–69. https://doi.org/10.1080/01932691.2020.1723620.
[6] Tian Y, Wang L, Tang Y, Liu C, Ma C, Wang T. Research and application of nano polymer microspheres diversion technique of deep fluid. Soc Pet Eng - SPE Int Oilf Nanotechnol Conf 2012;2012(2):261–6. https://doi.org/10.2118/156999-ms.
[7] Abdulbaki M, Huh C, Sepehrnoori K, Delshad M, Varavei A. A critical review on use of polymer microgels for conformance control purposes. J Pet Sci Eng 2014;122:741–53. https://doi.org/10.1016/j.petrol.2014.06.034.
[8] Cozic C, Rousseau D, Tabary R. Novel insights into microgel systems for water control. SPE Prod Oper 2009;24:590–601. https://doi.org/10.2118/115974-PA.
[9] Jia Hu, Ren Q, Pu W-F, Zhao J. Swelling mechanism investigation of microgel with double-cross-linking structures. Energy Fuels 2014;28(11):6735–44. https://doi.org/10.1021/ef5012325.
[10] He J, Shao M, Yue X, Yue T. Fabrication and characteristics of self-aggregation nanoparticles used for conformance control treatment. Polym Adv Technol 2021;32(1):190–201. https://doi.org/10.1002/pat.v32.110.1002/pat.5074.
[11] Qiu Y, Wei M, Bai B, Mao C. Data analysis and application guidelines for the microgel field applications. Fuel 2017;210:557–68. https://doi.org/10.1016/j.fuel.2017.08.094.
[12] Geng J, Ding H, Han Pu, Wu Y, Bai B. Transportation and Potential Enhanced Oil Recovery Mechanisms of Nanogels in Sandstone. Energy Fuels 2018;32(8):8358–65. https://doi.org/10.1021/acs.energyfuels.8b01873.
[13] Yao C, Lei G, Li L, Gao X. Selectivity of pore-scale elastic microspheres as a novel profile control and oil displacement agent. Energy Fuels 2012;26(8):5092–101. https://doi.org/10.1021/ef300689c.
[14] Liang T, Hou J, Qu M, Wen Y, Zhang W, Wu W, et al. The EOR mechanism and flow behaviors of high-viscosity modified starch nanogel particles in porous media. Soc Pet Eng - SPE/IATMI Asia Pacific Oil Gas Conf Exhib 2019, APOG 2019 2019. https://doi.org/10.2118/196414-ms.

[15] Liu C, Liao X, Zhang Y, Chang MM, Mu C, Li T, et al. Field application of polymer microspheres flooding: A pilot test in offshore heavy oil reservoir. Proc - SPE Annu Tech Conf Exhib 2012;1:813–8. https://doi.org/10.2118/158293-ms.

[16] Yao C, Xu X, Wang D, Lei G, Xue S, Hou J, et al. Research and application of micron-size polyacrylamide elastic microspheres as a smart sweep improvement and profile modification agent. SPE - DOE Improv Oil Recover Symp Proc 2016; 2016-Janua. https://doi.org/10.2118/179531-ms.

[17] Yao C, Lei G, Hou J, Xu X, Wang D, Steenhuis TS. Enhanced Oil Recovery Using Micron-Size Polyacrylamide Elastic Microspheres: Underlying Mechanisms and Displacement Experiments. Ind Eng Chem Res 2015;54(43):10925–34. https://doi.org/10.1021/acs.iecr.5b02717.

[18] Chang Y-S. Preparation and characterization of water-absorbent poly(arylamide-co-acrylic acid salt)'s. Lehigh University 1991.

[19] de Jong SJ, van Eerdenbrugh B, van Nostrum CF, Kettenes-van den Bosch JJ, Hennink WE. Physically crosslinked dextran hydrogels by stereocomplex formation of lactic acid oligomers: Degradation and protein release behavior. J Control Release 2001;71(3):261–75. https://doi.org/10.1016/S0168-3659(01)00228-0.

[20] Said HM, Abd Alla SG, El-Naggar AWM. Synthesis and characterization of novel gels based on carboxymethyl cellulose/acrylic acid prepared by electron beam irradiation. React Funct Polym 2004;61(3):397–404. https://doi.org/10.1016/j.reactfunctpolym.2004.07.002.

[21] Kadlubowski S. Radiation-induced synthesis of nanogels based on poly(N-vinyl-2-pyrrolidone)-A review. Radiat Phys Chem 2014;102:29–39. https://doi.org/10.1016/j.radphyschem.2014.04.016.

[22] Okubo M, Shiozaki M, Tsujihiro M, Tsukuda Y. Preparation of micron-size monodisperse polymer particles by seeded polymerization utilizing the dynamic monomer swelling method. Colloid Polym Sci 1991;269(3):222–6. https://doi.org/10.1007/BF00665495.

[23] Candau F, Leong YS, Pouyet G, Candau S. Inverse microemulsion polymerization of acrylamide: Characterization of the water-in-oil microemulsions and the final microlatexes. J Colloid Interface Sci 1984;101(1):167–83. https://doi.org/10.1016/0021-9797(84)90017-1.

[24] Guo JS, Sudol ED, Vanderhoff JW, El-Aasser MS. Particle nucleation and monomer partitioning in styrene O/W microemulsion polymerization. J Polym Sci, Part A: Polym Chem 1992;30:691–702. https://doi.org/10.1002/pola.1992.080300501.

[25] Geng J, Pu J, Wang L, Bai B. Surface charge effect of nanogel on emulsification of oil in water for fossil energy recovery. Fuel 2018;223:140–8. https://doi.org/10.1016/j.fuel.2018.03.046.

[26] Wang H, Lin M, Chen D, Dong Z, Yang Z, Zhang J. Research on the rheological properties of cross-linked polymer microspheres with different microstructures. vol. 331. Elsevier B.V; 2018. https://doi.org/10.1016/j.powtec.2018.03.045.

[27] Liu L, Gou S, Fang S, He Y, Tang L. Organic-inorganic microspheres of temperature-controlled size for profile control. J Mol Liq 2020;317:113993. https://doi.org/10.1016/j.molliq.2020.113993.

[28] Yang H, Kang W, Tang X, Gao Y, Zhu Z, Wang P, et al. Gel kinetic characteristics and creep behavior of polymer microspheres based on bulk gel. J Dispers Sci Technol 2018;39(12):1808–19. https://doi.org/10.1080/01932691.2018.1462192.

[29] Almahfood M, Bai B. Characterization and oil recovery enhancement by a polymeric nanogel combined with surfactant for sandstone reservoirs. Pet Sci 2021;18(1):123–35. https://doi.org/10.1007/s12182-020-00525-y.

[30] He J, Yue X, Sun Y, Feng X, Tan X. Preparation of uniform poly (Acrylamide-co-DVB) microspheres in a low toxicity solvent by dispersion polymerization. Aust J Chem 2015;68:1276–81. https://doi.org/10.1071/CH14670.

[31] Wang Z, Lin M, Xiang Y, Zeng T, Dong Z, Zhang J, et al. Zr-Induced Thermostable Polymeric Nanospheres with Double-Cross-Linked Architectures for Oil Recovery. Energy Fuels 2019;33(10):10356–64. https://doi.org/10.1021/acs.energyfuels.9b01463.

[32] Wang S, Tang Z, Qu J, Wu T, Liu Y, Wang J, et al. Research on the mechanisms of polyacrylamide nanospheres with different size distributions in enhanced oil recovery. RSC Adv 2021;11(10):5763–72. https://doi.org/10.1039/D0RA09348C.

[33] Yang H, Kang W, Yu Y, Yin X, Wang P, Zhang X. A new approach to evaluate the particle growth and sedimentation of dispersed polymer microsphere profile control system based on multiple light scattering. Powder Technol 2017;315:477–85. https://doi.org/10.1016/j.powtec.2017.04.001.

[34] Zhang P, Bai S, You Q, Ji W, Yu H, Li D. Preparation and properties of novel pH-sensitive core−shell microspheres for enhanced oil recovery. Polym Int 2017;66(9):1312–7. https://doi.org/10.1002/pi.2017.66.issue-910.1002/pi.5390.

[35] Liu J, Li L, Xu Z, Chen J, Dai C. Self-growing Hydrogel Particles with Applications for Reservoir Control: Growth Behaviors and Influencing Factors. J Phys Chem B 2021;125(34):9870–8. https://doi.org/10.1021/acs.jpcb.1c0528910.1021/acs.jpcb.1c05289.s001.

[36] Zhu D, Hou J, Chen Y, Zhao S, Bai B. In Situ Surface Decorated Polymer Microsphere Technology for Enhanced Oil Recovery in High-Temperature Petroleum Reservoirs. Energy Fuels 2018;32(3):3312–21. https://doi.org/10.1021/acs.energyfuels.8b00001.

[37] Yu Z, Li Y, Sha Ou, Su Z, Zhou W. Synthesis and properties of amphiprotic polyacrylamide microspheres as water shutoff and profile control. J Appl Polym Sci 2016;133(17):n/a–. https://doi.org/10.1002/app.43366.

[38] Meng G. Synthesis and Characterization of Polyacrylamide Microsphere with High Mechanical Strength. China University of Petroleum-Beijing; 2019.

[39] Zhang F. Applicaiont and Research of Deep Profile Control and Oil Displacement Technology of Polymer Microspheres in Low permeability Reservoirs. Xi'an Shiyou University, 2019.

[40] Du D-J, Pu W-F, Zhang S, Jin F-Y, Wang S-K, Ren F. Preparation and migration study of graphene oxide-grafted polymeric microspheres: EOR implications. J Pet Sci Eng 2020;192:107286. https://doi.org/10.1016/j.petrol.2020.107286.

[41] Tang X, Kang W, Zhou B, Gao Y, Cao C, Guo S, et al. Characteristics of composite microspheres for in-depth profile control in oilfields and the effects of polymerizable silica nanoparticles. Powder Technol 2020;359:205–15. https://doi.org/10.1016/j.powtec.2019.09.070.

[42] Zhu D, Bai B, Hou J. Polymer Gel Systems for Water Management in High-Temperature Petroleum Reservoirs: A Chemical Review. Energy Fuels 2017;31(12):13063–87. https://doi.org/10.1021/acs.energyfuels.7b02897.

[43] Li J, Niu L, Wu W, Sun M. The reservoir adaptability and oil displacement mechanism of polymer microspheres. Polymers (Basel) 2020;12:1–19. https://doi.org/10.3390/POLYM12040885.

[44] Balaceanu A, Demco DE, Möller M, Pich A. Heterogeneous morphology of random copolymer microgels as reflected in temperature-induced volume transition and 1H high-resolution transverse relaxation NMR. Macromol Chem Phys 2011;212(22):2467–77. https://doi.org/10.1002/macp.201100340.

[45] Chen X, Li Y, Liu Z, Li X, Zhang J, Zhang H. Core- and pore-scale investigation on the migration and plugging of polymer microspheres in a heterogeneous porous media. J Pet Sci Eng 2020;195:107636. https://doi.org/10.1016/j.petrol.2020.107636.

[46] Wang Z, Lin M, Jin S, Yang Z, Dong Z, Zhang J. Combined flooding systems with polymer microspheres and nonionic surfactant for enhanced water sweep and oil displacement efficiency in heterogeneous reservoirs. J Dispers Sci Technol 2020;41(2):267–76. https://doi.org/10.1080/01932691.2019.1570850.

[47] Wang Bo, Lin M, Guo J, Wang D, Xu F, Li M. Plugging properties and profile control effects of crosslinked polyacrylamide microspheres. J Appl Polym Sci 2016;133(30). https://doi.org/10.1002/app.43666.

[48] Schulte J, Pütz T, Gebhardt R. Statistical analysis of the swelling process of casein microparticles based on single particle measurements. Food Hydrocoll Heal 2021;1:100014. https://doi.org/10.1016/j.fhfh.2021.100014.

[49] Zhao S, Pu W, Wei B, Xu X. A comprehensive investigation of polymer microspheres (PMs) migration in porous media: EOR implication. Fuel 2019;235:249–58. https://doi.org/10.1016/j.fuel.2018.07.125.

[50] Weihs TP, Nawaz Z, Jarvis SP, Pethica JB. Limits of imaging resolution for atomic force microscopy of molecules. Appl Phys Lett 1991;59(27):3536–8. https://doi.org/10.1063/1.105649.

[51] Babu R, Singh E. Atomic Force Microscopy: A Source of Investigation in Biomedicine. Int J Electron Electr Eng 2014;7:59–66.

[52] Zhang L, Abbaspourrad A, Parsa S, Tang J, Cassiola F, Zhang M, et al. Core-Shell Nanohydrogels with Programmable Swelling for Conformance Control in Porous Media. ACS Appl Mater Interfaces 2020;12(30):34217–25. https://doi.org/10.1021/acsami.0c0995810.1021/acsami.0c09958.s001.

[53] Kesselman LRB, Shinwary S, Selvaganapathy PR, Hoare T. Synthesis of monodisperse, covalently cross-linked, degradable "smart" microgels using microfluidics. Small 2012;8(7):1092–8. https://doi.org/10.1002/smll.201102113.

[54] Lenchenkov N. Conformance Control in Heterogeneous Oil Reservoirs with Polymer Gels and Nano-Spheres. Delft University of Technology; 2017.

[55] Bai X. Preparation and application of deep modifier polymer microspheres. Northwest University 2019.

[56] Lei W, Xie C, Wu T, Wu X, Wang M. transport mechanism of deformable micro-gel particle through micropores with mechanical properties characterized by AFM. Sci Rep 2019;9(1). https://doi.org/10.1038/s41598-018-37270-7.

[57] Li Z, Zhao T, Lv W, Ma Bo, Hu Q, Ma X, et al. Nanoscale Polyacrylamide Copolymer/Silica Hydrogel Microspheres with High Compressive Strength and Satisfactory Dispersion Stability for Efficient Profile Control and Plugging. Ind Eng Chem Res 2021;60(28):10193–202. https://doi.org/10.1021/acs.iecr.1c0161710.1021/acs.iecr.1c01617.s001.

[58] Sun Z, Wang X, Kang X. The Reservoir Adaptability Evaluation and Oil Displacement Mechanism of a Novel Particle-Type Polymer Flooding Technology. Available SSRN 3898483 2021.

[59] Jin F, Yang L, Li X, Song S, Du D. Migration and plugging characteristics of polymer microsphere and EOR potential in produced-water reinjection of offshore heavy oil reservoirs. Chem Eng Res Des 2021;172:291–301. https://doi.org/10.1016/j.cherd.2021.06.018.

[60] Zhe S. Research on the evaluation method of polymer microsphere reservoir adaptability and the profile control and displacement mechanism. Northeast Petroleum University, n.d.

[61] Pu W, Zhao S, Wang S, Wei B, Yuan C, Li Y. Investigation into the migration of polymer microspheres (PMs) in porous media: Implications for profile control and oil displacement. Colloids Surf A Physicochem Eng Asp 2018;540:265–75. https://doi.org/10.1016/j.colsurfa.2018.01.018.

[62] Jia Y, Yang H, Cheng C, Li Z, Hou G, Yuan X, et al. Field application and performance evaluation of polymer microsphere profile control in low permeability oil reservoir. Soc Pet Eng - Abu Dhabi Int Pet Exhib Conf 2019, ADIP 2019 2019:1–12. https://doi.org/10.2118/197198-ms.

[63] Hua Z, Lin M, Dong Z, Li M, Zhang G, Yang J. Study of deep profile control and oil displacement technologies with nanoscale polymer microspheres. J Colloid Interface Sci 2014;424:67–74. https://doi.org/10.1016/j.jcis.2014.03.019.

[64] Du D-J, Pu W-F, Jin F, Hou D-D, Shi Le. Experimental investigation on plugging and transport characteristics of Pore-Scale microspheres in heterogeneous porous

media for enhanced oil recovery. J Dispers Sci Technol 2021;42(8):1152–62. https://doi.org/10.1080/01932691.2020.1729796.
[65] Liu J, Zhang Y, Li X, Dai L, Li H, Xue B, et al. Experimental Study on Injection and Plugging Effect of Core-Shell Polymer Microspheres: Take Bohai Oil Reservoir as an Example. ACS Omega 2020;5(49):32112–22. https://doi.org/10.1021/acsomega.0c05252.
[66] Zhao W, Ni J, Hou G, Jia Y, Diwu P, Yuan X, et al. Research on optimal blocking limits and injection parameter optimization of polymer microsphere conformance control. ACS Omega 2021;6(12):8297–307. https://doi.org/10.1021/acsomega.1c00009.
[67] Zhang Y, Geng J, Liu J, Bai B, He X, Wei M, et al. Direct pore-level visualization and verification of in situ oil-in-water pickering emulsification during polymeric nanogel flooding for EOR in a transparent three-dimensional micromodel. Langmuir 2021;37(45):13353–64. https://doi.org/10.1021/acs.langmuir.1c02029.
[68] Aufderhorst-Roberts A, Baker D, Foster RJ, Cayre O, Mattsson J, Connell SD. Nanoscale mechanics of microgel particles. Nanoscale 2018;10(34):16050–61. https://doi.org/10.1039/C8NR02911C.
[69] Mercadé-Prieto R, Zhang Z. Mechanical characterization of microspheres capsules, cells and beads: A review. J Microencapsul 2012;29(3):277–85. https://doi.org/10.3109/02652048.2011.646331.
[70] Liu T, Donald AM, Zhang Z. Novel manipulation in environmental scanning electron microscope for measuring mechanical properties of single nanoparticles. Mater Sci Technol 2005;21(3):289–94. https://doi.org/10.1179/174328405X29230.
[71] Yan Y, Zhang Z, Stokes JR, Zhou Q-Z, Ma G-H, Adams MJ. Mechanical characterization of agarose micro-particles with a narrow size distribution. Powder Technol 2009;192(1):122–30. https://doi.org/10.1016/j.powtec.2008.12.006.
[72] Yang H, Shao S, Zhu T, Chen C, Liu S, Zhou B, et al. Shear resistance performance of low elastic polymer microspheres used for conformance control treatment. J Ind Eng Chem 2019;79:295–306. https://doi.org/10.1016/j.jiec.2019.07.005.
[73] Larsson M, Hill A, Duffy J. Suspension stability: Why particle size, zeta potential and rheology are important Product Technical Specialists Rheometry Products Malvern Instruments Limited. Annu Trans Nord Rheol Soc 2012:1999.
[74] Clogston JD, Patri AK. Zeta Potential Measurement BT - Characterization of Nanoparticles Intended for Drug Delivery. In: McNeil SE, editor., Totowa, NJ: Humana Press; 2011, p. 63–70. https://doi.org/10.1007/978-1-60327-198-1_6.
[75] Sun X, Zhang Y, Chen G, Gai Z. Application of nanoparticles in enhanced oil recovery: A critical review of recent progress. Energies 2017;10(3):345. https://doi.org/10.3390/en10030345.
[76] Pate K, Safier P. 12 - Chemical metrology methods for CMP quality. In: Babu SBT-A in CMP (CMP), editor., Woodhead Publishing; 2016, p. 309–11. https://doi.org/https://doi.org/10.1016/B978-0-08-100165-3.00012-7.
[77] Zhang Z. Research on Synthesis and Profile Control Properties of Pore-scale Polymer Microspheres. China University of Petroleum-East China 2008.
[78] Wu X. Synthesis and Properties of Polyacrylamide Copolymer Microspheres. Tianjin University, 2014.
[79] Zhu Q. Verse emulsion polymerization method-the evaluation of microsphere for conformance control. Southwest Petroleum University, n.d.
[80] Liu Z. Research and application of polymer microsphere in plugging and controlling water in horizontal wells. Southwest Petroleum University; 2018.
[81] Chauveteau G, Tabary R, Blin N, Renard M, Rousseau D, Faber R. Disproportionate permeability reduction by soft preformed microgels. Proc - SPE Symp Improv Oil Recover 2004;2004-April. https://doi.org/10.2118/89390-ms.
[82] Feng Y, Tabary R, Renard M, Le BC, Omari A, Chauveteau G. Characteristics of Microgels Designed for Water Shutoff and Profile Control. SPE Int Symp Oilf Chem 2003:19–26. https://doi.org/10.2523/80203-ms.
[83] Salunkhe B, Schuman T, Al Brahim A, Bai B. Ultra-high temperature resistant preformed particle gels for enhanced oil recovery. Chem Eng J 2021;426:130712. https://doi.org/10.1016/j.cej.2021.130712.
[84] You Z, Aji K, Badalyan A, Bedrikovetsky P. Effect of nanoparticle transport and retention in oilfield rocks on the efficiency of different nanotechnologies in oil industry. OnePetro: SPE Int. Oilf. Nanotechnol. Conf. Exhib; 2012.
[85] Ding H. Factors impacting the transport and enhanced oil recovery potential of polymeric nanogel in sandstone. Missouri University of Science and Technology; 2020.
[86] Yuan C, Pu W, Varfolomeev MA, Wei J, Zhao S, Cao LN. Deformable microgel for enhanced oil recovery in high-temperature and ultrahigh-salinity reservoirs: How to design the particle size of microgel to achieve its optimal match with pore throat of porous media. SPE J 2021;26:2053–67. https://doi.org/10.2118/197804-PA.
[87] Cao D, Han M, Wang J, Alshehri AJ. Polymeric microsphere injection in large pore-size porous media. Petroleum 2020;6(3):264–70. https://doi.org/10.1016/j.petlm.2020.03.002.
[88] Shi X, Yue X. Migration and plugging mechanisms of self-aggregated microspheres as a novel profile control. J Pet Sci Eng 2020;184:106458. https://doi.org/10.1016/j.petrol.2019.106458.
[89] Nie X, Chen J, Cao Yi, Zhang J, Zhao W, He Y, et al. Investigation on plugging and profile control of polymer microspheres as a displacement fluid in enhanced oil recovery. Polymers (Basel) 2019;11(12):1993. https://doi.org/10.3390/polym11121993.
[90] Cao D, Han M, Wang J, AlSofi A. Optimization of microsphere injection by balancing the blocking and migration capacities in a heterogeneous carbonate matrix. Soc Pet Eng - Abu Dhabi Int Pet Exhib Conf 2020, ADIP 2020 2020;mic. https://doi.org/10.2118/203131-ms.
[91] Han Pu, Geng J, Ding H, Zhang Ye, Bai B. Experimental study on the synergistic effect of nanogel and low salinity water on enhanced oil recovery for carbonate reservoirs. Fuel 2020;265:116971. https://doi.org/10.1016/j.fuel.2019.116971.
[92] Yang H, Kang W, Yin X, Tang X, Song S, Lashari ZA, et al. Research on matching mechanism between polymer microspheres with different storage modulus and pore throats in the reservoir. Powder Technol 2017;313:191–200. https://doi.org/10.1016/j.powtec.2017.03.023.
[93] Yao C, Liu B, Li L, Zhang K, Lei G, Steenhuis TS. Transport and retention behaviors of deformable polyacrylamide microspheres in convergent-divergent microchannels. Environ Sci Technol 2020;54(17):10876–84. https://doi.org/10.1021/acs.est.0c0224310.1021/acs.est.0c02243.s001.
[94] Chen X, Li Y, Liu ZY, Zhang J, Chen C, Ma M. Investigation on matching relationship and plugging mechanism of self-adaptive micro-gel (SMG) as a profile control and oil displacement agent. Powder Technol 2020;364:774–84. https://doi.org/10.1016/j.powtec.2020.02.027.
[95] Li J, Niu L, Lu X. Migration characteristics and deep profile control mechanism of polymer microspheres in porous media. Energy Sci Eng 2019;7(5):2026–45. https://doi.org/10.1002/ese3.v7.510.1002/ese3.409.
[96] El-Diasty AI, Aly AM. Understanding the mechanism of nanoparticles applications in enhanced oil recovery. Soc Pet Eng - SPE North Africa Tech Conf Exhib 2015. NATC 2015;2015(000):944–62. https://doi.org/10.2118/175806-ms.
[97] Skauge T, Spildo K, Skauge A. Nano-sized particles for EOR. SPE - DOE Improv Oil Recover Symp Proc 2010;2:1281–90. https://doi.org/10.2523/129933-ms.
[98] Hua Z, Lin M, Guo J, Xu F, Li Z, Li M. Study on plugging performance of cross-linked polymer microspheres with reservoir pores. J Pet Sci Eng 2013;105:70–5. https://doi.org/10.1016/j.petrol.2013.03.008.
[99] Li S, Yu H, Li T-D, Chen Zi, Deng W, Anbari A, et al. Understanding transport of an elastic, spherical particle through a confining channel. Appl Phys Lett 2020;116(10):103705. https://doi.org/10.1063/1.5139887.
[100] Yao C, Lei G, Cathles LM, Steenhuis TS. Pore-scale investigation of micron-size polyacrylamide elastic microspheres (MPEMs) transport and retention in saturated porous media. Environ Sci Technol 2014;48(9):5329–35. https://doi.org/10.1021/es500077s.
[101] Han P, Geng J, Bai B. Investigation on transport behavior of nanogel in low permeable porous medium. J Pet Sci Eng 2019;178:999–1005. https://doi.org/10.1016/j.petrol.2019.04.020.
[102] Dai C, Liu Y, Zou C, You Q, Yang S, Zhao M, et al. Investigation on matching relationship between dispersed particle gel (DPG) and reservoir pore-throats for in-depth profile control. Fuel 2017;207:109–20. https://doi.org/10.1016/j.fuel.2017.06.076.
[103] Wu T, Zhao Y, Song Z, Sun Y. Research on New Polymer Microsphere Gel for In-Depth Profile Control and Its Application in Low Permeability Reservoir, vol. 2. Singapore: Springer; 2021. 10.1007/978-981-16-0761-5_282.
[104] Almohsin A, Bai B, Imqam A, Wei M, Kang W, Delshad M, et al. Transport of nanogel through porous media and its resistance to water flow. Proc - SPE Symp Improv Oil Recover 2014;2:692–705. https://doi.org/10.2118/169078-ms.
[105] Imqam A, Bai B, Al Ramadan M, Wei M, Delshad M, Sepehrnoori K. Preformed-particle-gel extrusion through open conduits during conformance-control treatments. SPE J 2015;20:1083–93. https://doi.org/10.2118/169107-PA.
[106] Zhang H, Bai B. Preformed-particle-gel transport through open fractures and its effect on water flow. SPE J 2011;16:388–400. https://doi.org/10.2118/129908-pa.
[107] Li S, Yu HH, Fan J. Modeling transport of soft particles in porous media. Phys Rev E 2021;104:1–9. https://doi.org/10.1103/PhysRevE.104.025112.
[108] Petosa AR, Jaisi DP, Quevedo IR, Elimelech M, Tufenkji N. Aggregation and deposition of engineered nanomaterials in aquatic environments: Role of physicochemical interactions. Environ Sci Technol 2010;44(17):6532–49. https://doi.org/10.1021/es100598h.
[109] McDowell-boyer LM, Hunt JR, Itar N. Particle transport through porous media 1986;22:1901–21.
[110] Zhang T. Modeling of nanoparticle transport in porous media 2012.
[111] Ryan JN, Elimelech M. Colloid mobilization and transport in groundwater. Colloids Surfaces A Physicochem Eng Asp 1996;107:1–56. https://doi.org/10.1016/0927-7757(95)03384-X.
[112] Rousseau D, Chauveteau G, Renard M, Tabary R, Zaitoun A, Mallo P, et al. Rheology and transport in porous media of new water shutoff/conformance control microgels. SPE Int Symp Oilf Chem Proc 2005. https://doi.org/10.2523/93254-ms.
[113] Chauveteau G, Tabary R, le Bon C, Renard M, Feng Y, Omari A. In-Depth Permeability Control by Adsorption of Soft Size-Controlled Microgels. SPE - Eur Form Damage Conf Proceedings, EFDC 2003. https://doi.org/10.2523/82228-ms.
[114] Li S. Study on Plugging and Migration of Cross-linked Polymer Microspheres. China University of Petroleum-Beijing; 2016.
[115] Zhang T, Murphy MJ, Yu H, Bagaria HG, Yoon KY, Neilson BM, et al. Investigation of nanoparticle adsorption during transport in porous media. SPE J 2015;20:667–77. https://doi.org/10.2118/166346-PA.
[116] Yu H. Transport and retention of surface-modified nanoparticles in sedimentary rocks 2012.
[117] Nikita Sergeevich Lenchenkov. Conformance Control in Heterogeneous Oil Reservoirs with Polymer Gels and Nano Spheres. Delft University of Technology 2017. https://doi.org/10.4233/uuid.
[118] Wyss HM, Franke T, Mele E, Weitz DA. Capillary micromechanics: Measuring the elasticity of microscopic soft objects. Soft Matter 2010;6:4550–5. https://doi.org/10.1039/c003344h.

[119] Bai B, Liu Y, Coste JP, Li L. Preformed particle gel for conformance control: Transport mechanism through porous media. Proc - SPE Symp Improv Oil Recover 2004;2004-April. https://doi.org/10.2523/89468-ms.
[120] Chen L, Wang KX, Doyle PS. Effect of internal architecture on microgel deformation in microfluidic constrictions. Soft Matter 2017;13(9):1920–8. https://doi.org/10.1039/C6SM02674E.
[121] Krummel AT, Datta SS, Münster S, Weitz DA. Visualizing multiphase flow and trapped fluid configurations in a model three-dimensional porous medium. AIChE J 2013;59(3):1022–9.
[122] Sun Z, Kang X, Tang X, Wu X, Li Q, Wang Y, et al. Performance evaluation and field trial of self-adaptive microgel flooding technology. Soc Pet Eng - Abu Dhabi Int Pet Exhib Conf 2018, ADIPEC 2018 2019. https://doi.org/10.2118/192651-ms.
[123] Su Y, Li Y, Wang L, He Y. Experimental and pilot tests of deep profile control by injecting small slug-size nano-microsphere in offshore oil fields. Proc Annu Offshore Technol Conf 2019;2019-May. https://doi.org/10.4043/29452-ms.
[124] Lalehrokh F, Bryant SL, Huh C, Sharma MM. Application of pH-triggered polymers in fractured reservoirs to increase sweep efficiency. Proc - SPE Symp Improv Oil Recover 2008;3:1100–12.
[125] Spildo K, Skauge A, Aarra MG, Tweheyo MT. A new polymer application for North Sea reservoirs. SPE Reserv Eval Eng 2009;12:427–32. https://doi.org/10.2118/113460-PA.
[126] Ye Y, Wu X, Huang Z, Bi T, Yang Z, Wang X, et al. Mechanism experimental study on flooding control of soft microgel by low-field nuclear magnetic resonance. J Phys Conf Ser 2021;2011(1):012017. https://doi.org/10.1088/1742-6596/2011/1/012017.
[127] Zhou Y, Jiang H, Wang C, Li B. Experimental study of microscopic displacement efficiency of polymer microspheres using low-field NMR. J Dispers Sci Technol 2014;35(7):1003–8. https://doi.org/10.1080/01932691.2013.825569.
[128] Zhe Y. Study on profile-control flooding mechanism of polymer microsphere. Adv Fine Petrochemicals 2013;14:1–4.
[129] Kwok M, hin, Ngai T. A confocal microscopy study of micron-sized poly(N-isopropylacrylamide) microgel particles at the oil-water interface and anisotopic flattening of highly swollen microgel. J Colloid Interface Sci 2016;461:409–18. https://doi.org/10.1016/j.jcis.2015.09.049.
[130] Lei W, Liu T, Xie C, Yang H, Wu T, Wang M. Enhanced oil recovery mechanism and recovery performance of micro-gel particle suspensions by microfluidic experiments. Energy Sci Eng 2020;8(4):986–98. https://doi.org/10.1002/ese3.v8.410.1002/ese3.563.
[131] Pritchett J, Frampton H, Brinkman J, Cheung S, Morgan J, Chang KT, et al. Field application of a new in-depth waterflood conformance improvement tool. Proc - SPE Int Improv Oil Recover Conf Asia Pacific 2003:365–72. https://doi.org/10.2118/84897-ms.
[132] Wasan DT, Nikolov AD. Spreading of nanofluids on solids. Nature 2003;423(6936):156–9. https://doi.org/10.1038/nature01591.
[133] Chengara A, Nikolov AD, Wasan DT, Trokhymchuk A, Henderson D. Spreading of nanofluids driven by the structural disjoining pressure gradient. J Colloid Interface Sci 2004;280(1):192–201. https://doi.org/10.1016/j.jcis.2004.07.005.
[134] Wasan D, Nikolov A, Kondiparty K. The wetting and spreading of nanofluids on solids: Role of the structural disjoining pressure. Curr Opin Colloid Interface Sci 2011;16(4):344–9. https://doi.org/10.1016/j.cocis.2011.02.001.
[135] Kondiparty K, Nikolov AD, Wasan D, Liu K. Dynamic Spreading of Nano fl uids on Solids. Part I: Experimental 2012.
[136] Liu K-L, Kondiparty K, Nikolov AD, Wasan D. Dynamic spreading of nanofluids on solids part II: Modeling. Langmuir 2012;28(47):16274–84. https://doi.org/10.1021/la302702g.
[137] ShamsiJazeyi H, Miller CA, Wong MS, Tour JM, Verduzco R. Polymer-coated nanoparticles for enhanced oil recovery. J Appl Polym Sci 2014;131(15):n/a–. https://doi.org/10.1002/app.40576.
[138] Zhang H, Nikolov A, Wasan D. Enhanced oil recovery (EOR) using nanoparticle dispersions: Underlying mechanism and imbibition experiments. Energy Fuels 2014;28(5):3002–9. https://doi.org/10.1021/ef500272r.
[139] Nazari Moghaddam R, Bahramian A, Fakhroueian Z, Karimi A, Arya S. Comparative study of using nanoparticles for enhanced oil recovery: Wettability alteration of carbonate rocks. Energy Fuels 2015;29(4):2111–9. https://doi.org/10.1021/ef5024719.
[140] Sefiane K, Skilling J, MacGillivray J. Contact line motion and dynamic wetting of nanofluid solutions. Adv Colloid Interface Sci 2008;138(2):101–20. https://doi.org/10.1016/j.cis.2007.12.003.
[141] Sharma T, Iglauer S, Sangwai JS. Silica Nanofluids in an Oilfield Polymer Polyacrylamide: Interfacial Properties, Wettability Alteration, and Applications for Chemical Enhanced Oil Recovery. Ind Eng Chem Res 2016;55(48):12387–97. https://doi.org/10.1021/acs.iecr.6b0329910.1021/acs.iecr.6b03299.s001.
[142] Kuang W, Saraji S, Piri M. A systematic experimental investigation on the synergistic effects of aqueous nanofluids on interfacial properties and their implications for enhanced oil recovery. Fuel 2018;220:849–70. https://doi.org/10.1016/j.fuel.2018.01.102.
[143] Zhao M, Cheng Y, Wu Y, Dai C, Gao M, Yan R, et al. Enhanced oil recovery mechanism by surfactant-silica nanoparticles imbibition in ultra-low permeability reservoirs. J Mol Liq 2022;348:118010. https://doi.org/10.1016/j.molliq.2021.118010.
[144] Kondiparty K, Nikolov A, Wu S, Wasan D. Wetting and spreading of nanofluids on solid surfaces driven by the structural disjoining pressure: statics analysis and experiments. Langmuir 2011;27(7):3324–35.
[145] Maghzi A, Mohebbi A, Kharrat R, Ghazanfari MH. Pore-Scale Monitoring of Wettability Alteration by Silica Nanoparticles During Polymer Flooding to Heavy Oil in a Five-Spot Glass Micromodel. Transp Porous Media 2011;87(3):653–64. https://doi.org/10.1007/s11242-010-9696-3.
[146] Geng J, Shi X, Han P, Wu Y, Bai B, Zhan J, et al. Experimental study on charged nanogels for interfacial tension reduction and emulsion stabilization at various salinities and oil types. Energy Fuels 2020;34(12):15894–904. https://doi.org/10.1021/acs.energyfuels.0c02591.
[147] Yakasai F, Jaafar MZ, Bandyopadhyay S, Agi A. Current developments and future outlook in nanofluid flooding: A comprehensive review of various parameters influencing oil recovery mechanisms. J Ind Eng Chem 2021;93:138–62. https://doi.org/10.1016/j.jiec.2020.10.017.
[148] Li K, Wang D, Jiang S. Review on enhanced oil recovery by nanofluids. Oil Gas. Sci Technol 2018;73. https://doi.org/10.1051/ogst/2018052.
[149] Hendraningrat L, Li S, Torsæter O. A coreflood investigation of nanofluid enhanced oil recovery. J Pet Sci Eng 2013;111:128–38. https://doi.org/10.1016/j.petrol.2013.07.003.
[150] Rezaei A, Khodabakhshi A, Esmaeili A, Razavifar M. Effects of initial wettability and different surfactant-silica nanoparticles flooding scenarios on oil-recovery from carbonate rocks. Petroleum 2021. https://doi.org/10.1016/j.petlm.2021.03.009.
[151] Giraldo J, Benjumea P, Lopera S, Cortés FB, Ruiz MA. Wettability alteration of sandstone cores by alumina-based nanofluids. Energy Fuels 2013;27(7):3659–65. https://doi.org/10.1021/ef4002956.
[152] Moradi B, Pourafshary P, Jalali Farahani F, Mohammadi M, Emadi MA. Application of SiO2 nano particles to improve the performance of water alternating gas EOR process. Soc Pet Eng - SPE Oil Gas India Conf Exhib 2015:1–8. https://doi.org/10.2118/178040-ms.
[153] Yuan W, Yang Y, Hou J, Chen T. Investigation on the profile control and oil displacement of combining nano-polymer microspheres and low salinity water flooding. Oilf Chem 2022;39:39–45.
[154] Idogun AK, Iyagba ET, Ukwotije-Ikwut RP, Aseminaso A. A review study of oil displacement mechanisms and challenges of nanoparticle enhanced oil recovery. Soc Pet Eng - SPE Niger Annu Int Conf Exhib 2016. https://doi.org/10.2118/184352-ms.
[155] Li S, Torsæter O. An Experimental Investigation of EOR Mechanisms for Nanoparticles Fluid in Glass Micromodel. Int Symp Soc Core Anal (Avignon / Fr 2014:1–12. https://doi.org/10.13140/RG.2.1.4181.3604.
[156] Luo D, Wang F, Alam MK, Yu F, Mishra IK, Bao J, et al. Colloidal Stability of Graphene-Based Amphiphilic Janus Nanosheet Fluid. Chem Mater 2017;29(8):3454–60. https://doi.org/10.1021/acs.chemmater.6b0514810.1021/acs.chemmater.6b05148.s001.